Nataly Andrea Pimiento Quiroga

Efeito da composição e configuração da paisagem urbana no serviço de regulação da qualidade do ar durante a quarentena da COVID-19

Effects of urban landscape composition and configuration on air quality regulation service during COVID-19's quarantine

Quiroga, Nataly Andrea Pimiento

Título: Efeito da composição e configuração da paisagem urbana no serviço de regulação da qualidade do ar durante a quarentena da COVID-19

São Paulo

2022

Nataly Andrea Pimiento Quiroga

Efeito da composição e configuração da paisagem urbana no serviço de regulação da qualidade do ar durante a quarentena da COVID-19

Effects of urban landscape composition and configuration on air quality regulation service during COVID-19's quarantine

Dissertação apresentada ao Instituto de Biociências da Universidade de São Paulo, para a obtenção de Título de Mestre em Ecologia na Área de Ecossistemas Terrestres.

Orientador: Jean Paul Metzger

Coorientadora: Paula Ribeiro Prist

São Paulo

2022

Ficha Catalográfica

Pimiento Quiroga, Nataly Andrea

Efeito da composição e configuração da paisagem urbana no serviço de regulação da qualidade do ar durante a quarentena da COVID-19 / Nataly Andrea Pimiento Quiroga; orientador Jean Paul Metzger; coorientadora Paula Ribeiro Prist -- São Paulo, 2022.

59 p.

Dissertação (Mestrado) -- Instituto de Biociências da Universidade de São Paulo. Programa de Pós-Graduação em Ecologia.

1. Áreas verdes. 2. Árvores urbanas. 3. Poluição do ar. 4. Regulação da qualidade do ar. 5. Serviços ecossistêmicos.

Comissão Julgadora:

_____ _____

Prof(a). Dr(a). Prof(a). Dr(a).

_____

Prof(a). Dr.(a).

Orientador(a)

Dedicatória

À minha família na Colômbia

E a que ganhei aqui no Brasil...

Epígrafe

“A natureza introduziu grande variedade na paisagem, mas o homem demonstrou paixão por simplificá-la. Assim, ele desfaz os freios e contrapesos embutidos pelos quais a natureza mantém as espécies dentro de limites.”

Rachel Carson

" O medo é uma resposta de sobrevivência. O medo nos faz correr, nos faz pular, pode nos fazer agir sobre-humanos. Mas precisamos de um lugar para onde correr. Sem isso, o medo é apenas paralisante. Então, o verdadeiro truque, a única esperança, realmente, é permitir que o terror de um futuro inviável seja equilibrado e apaziguado pela perspectiva de construir algo muito melhor do que muitos de nós ousamos esperar."

Naomi Klein

Agradecimentos

Agradeço a Coordenação de Aperfeiçoamento de Pessoal de Nível Superior – Brasil (CAPES) – Código de Financiamento 88887.372809/2019-00, pela concessão da bolsa de mestrado que me permitiu realizar este projeto.

Ao meu orientador Jean Paul Metzger, por ter me dado autonomia no desenvolvimento do meu projeto, confiar em mim e me incentivar durante o processo.

À minha coorientadora Paula Prist, por sempre responder cada uma das minhas dúvidas, ter a paciência e disposição de me explicar, e até colocar a mão na massa para me ajudar.

Aos meus colegas do Lepac pelos momentos compartilhados, pela ajuda técnica e pelas discussões que fizemos ao redor deste trabalho.

À minha família pelo apoio, em especial a minha mãe, que tem sustentado este sonho desde o começo e que me deu asas para vir atrás dele.

À minha namorada por todo o apoio durante estes últimos dois anos, por me entender, me acompanhar e me incentivar nos momentos mais difíceis.

Contents

Resumo

As megacidades estão enfrentando o desafio de manter importantes serviços ecossistêmicos, incluindo o de regulação da qualidade do ar. Espaços verdes urbanos são potenciais fornecedores deste serviço e aparentam ser uma solução eficaz baseada na natureza. Porém, até o momento, a maior parte dos estudos tem focado principalmente em aspetos da composição das áreas verdes, deixando de lado como a configuração espacial — particularmente a fragmentação — poderia afetar a regulação da qualidade do ar. Também é escasso o conhecimento sobre como a provisão desse serviço varia com potenciais diminuições nas emissões de poluentes, como a que ocorreu com a quarentena estabelecida pela pandemia do COVID-19. Neste trabalho, tentamos preencher essas lacunas de conhecimento, investigando qual a contribuição das áreas verdes urbanas na redução da poluição do ar, e em qual configuração esse serviço é otimizado, nos períodos antes, durante e após a quarentena estabelecida pela pandemia em uma das maiores cidades do hemisfério Sul (São Paulo, Brasil). Consideramos explicitamente a oferta, demanda e os fluxos relacionados à prestação de serviços ecossistêmicos. Fizemos uma seleção de modelos usando as concentrações horárias de poluentes (CO, NO_2, PM2.5 e PM10) como variável resposta, enquanto foram usadas como variáveis preditoras a quantidade, densidade e velocidade de deposição seca de áreas verdes (relacionadas à oferta); a quantidade de emissões de veículos (como indicador de demanda); diferentes escalas espaciais (associadas ao fluxo); configuração de áreas verdes; e variáveis meteorológicas. Nossos resultados mostraram que áreas com maior cobertura arbórea e menos emissões veiculares diminuíram as concentrações de CO, NO_2 e PM. O efeito das áreas verdes na redução dos poluentes atmosféricos foi maior nos períodos de menor demanda (início da quarentena), chegando a ser duas vezes maior para NO_2 e três vezes maior para PM10, em comparação com períodos de maior demanda (antes e após a quarentena). Além disso, a fragmentação dos espaços arborizados, que proporciona maior proximidade aos locais de emissão de poluentes (porém com manchas menores de áreas verdes), tende a diminuir as concentrações de PM10 e aumentar as concentrações de PM2.5, CO e NO_2. Estas relações foram observadas em escalas entre 500 e 1000 m, mas os fluxos de poluentes podem ser ainda mais amplos, indicando que a interação entre as áreas de oferta e demanda em áreas urbanas pode ocorrer em grandes extensões espaciais. Nossos resultados demonstram que para aumentar o serviço de regulação do ar oferecido pela vegetação, seria importante maximizar a quantidade de cobertura arbórea (mesmo longe das áreas poluidoras) e minimizar sua fragmentação, além de reduzir as emissões veiculares.

Palavras chave: áreas verdes, árvores urbanas, poluição do ar, regulação da qualidade do ar, serviços ecossistêmicos.

Abstract

Megacities are currently facing the challenge of maintaining important ecosystem services, such as air quality regulation. Urban greenspaces are potential suppliers of this ecosystem service, and thus appear to be an effective nature-based solution. However, the knowledge compiled so far has focused mainly on the composition aspects of these areas, while few studies assess how the spatial configuration of green areas, in particular fragmentation, affects air quality regulation. Even less is known about how this service varies with decreasing pollutant emissions resulting from the quarantine of the COVID pandemic. Here we fill these research gaps by testing the contribution and best configuration of green areas in reducing air pollution, before, during, and after a quarantine period, in one of the largest cities of the Global South (São Paulo, Brazil). We explicitly considered the supply, demand and flows related to this ecosystem service provision. We relied on a model selection approach using hourly concentrations of different pollutants (CO, NO2, $PM_{2.5,}$ and $PM_{10,}$) as the response variable. The amount, density and dry deposition velocity of greenspaces (related to supply), amount of vehicle emissions (proxy of demand), different spatial scales (proxy of flow), greenspaces configuration, and meteorological variables were used as predictors. Our results showed that areas with higher tree cover, and less vehicular emissions decreased concentrations of CO, NO2 and PM. The effect of green areas in the reduction of air pollutants was higher in periods of lower demand (start of quarantine), almost doubling in the case of NO2 and even tripling, in the case of PM10, when compared to periods of higher demand (before and after quarantine). Furthermore, fragmented configuration that provided greater proximity of green areas to pollutant emission sites, but with smaller green areas, tended to decrease PM10 concentrations, while increasing PM2.5, CO and NO2 concentrations. These relationships were observed for scales from 500 to 1000 m, but the pollutant flows could be even wider, indicating that the interaction between supply and demand in urban areas can occur over very large spatial extents. Our results demonstrate that to enhance the air regulation service offered by vegetation, it would be important to maximize the amount of tree cover, even if distant from pollution source areas, and minimize its fragmentation, beyond the reduction of vehicular emissions.

Key words: green areas, urban trees, air pollution, air quality regulation, ecosystem services.

1 INTRODUCTION

With the global increase in urbanization, a growing proportion of human population is subject to environmental problems related to urban areas, such as waste management, traffic flow, flood risk, urban heat island effect and air quality impoverishment (CHOURABI *et al.*, 2012; LIVESLEY; MCPHERSON; CALFAPIETRA, 2016). This situation makes urgent the adoption of sustainable measures to reduce and mitigate the negative impacts of urbanization, through the provision of urban landscape services.

Among the main environmental issues, air pollution is of great concern because more than 80% of the people who live in urban areas are exposed to pollution levels above acceptable limits, causing approximately 7 million deaths annually (WHO 2020). Pollution is mainly produced through fossil combustion, which contribute to the release of nitrogen oxides (NO), sulphur oxides (SO), carbon monoxide (CO), ozone (O3), and of solid and liquid contaminant particles called “particle matter” (POPESCU; IONEL, 2010). These air pollutants are related to human morbidity and mortality increase, depending on their dose and time of exposure. Increased levels of SO and NO can cause bronchoconstriction and dyspnea in asthmatic patients. Particulate matter and O3 penetrate in the alveolar epithelium and cause lung inflammation along with systemic inflammatory changes that affect blood coagulation (KAMPA; CASTANAS, 2008). Finally, high concentrations of CO reduce oxygen availability, affecting the function of different organs (RIEDIKER *et al.*, 2004).

Vehicular emissions are one of the main contributors to global air pollution along with heat production, agriculture, and industry activities (IPCC, 2014; KUMAR *et al.*, 2021), accounting for 14% of global greenhouse gas emissions (IPCC, 2014) and for 8% of PM2.5 (WEAGLE *et al.*, 2018). Even though policies have been established to reduce vehicular emissions, the continuous growth in urbanization has led to an increase in the vehicle fleet, and consequently in pollutants emissions (KUMAR *et al.*, 2021). However, during 2020, with the social distance policy adopted around the world to face COVID-19, it was observed a global reduction in pollutants emissions (LOH *et al.*, 2021). Despite the environmental gains during the isolation period due to industry

shutdowns, lockdowns and travel restrictions, there were also global losses in income and employment (LENZEN *et al.*, 2020), which impede this kind of measure from being a pragmatic solution for the air pollution problem.

Urban green spaces are known for contributing to the provision of several ecosystem services, including air quality regulation services (IRGA; BURCHETT; TORPY, 2015; ROY; BYRNE; PICKERING, 2012) and may be a key element to mitigate air pollution problems. The provision of air regulation service has three main components: supply (areas where pollutant deposition occurs); demand (amount of regulation needed to meet air quality standards), and flow (movement of pollutants from emission to deposition areas). However, frequently only one of these three components (most commonly, supply) is studied in the evaluation of ecosystem service provision (BARÓ *et al.*, 2016), which may lead to overestimations, and therefore not offer an accurate assessment of the effect of greenspaces in the provision of this ecosystem service (METZGER *et al.*, 2021).

Trees are recognized to reduce the air pollution effects of road traffic and industries in residential areas (KRZYŻANOWSKI; KUNA-DIBBERT; SCHNEIDER, 2005), with estimated economic benefits in human mortality reduction ranging from $1.1 to 60.1 million USD annually (NOWAK *et al.*, 2013). Vegetation does this through the dry deposition process, which reduces the concentration of pollutants through two main ways: (i) the interception and accumulation of particles (PM10 and PM2.5) on external surfaces, like leaf pubescence's and waxy surfaces (BECKETT; FREER-SMITH; TAYLOR, 2000); and (ii) through the capture of pollutant gases like O3, NO2, and CO, inside their stomata (CIESLIK; OMASA; PAOLETTI, 2009). Therefore, green areas can be considered a proxy, or an important part of the supply component. Generally, higher density and closed canopy covers are associated with a reduction in particulate matter concentrations (IRGA; BURCHETT; TORPY, 2015), because larger tree crowns have the potential to ameliorating air quality by maximizing pollutant deposition (PAOLETTI; KARNOSKY; PERCY, 2004). Thus, structural tree parameters, like density and crown continuity, and leaf area index have been suggested as indicators of this service's supply (ROELAND *et al.*, 2019). The quantity of these green areas is also important, with more extensive and continuous presenting better air quality outcomes (SHEN; LUNG, 2016).

However, the effect of green areas distribution, or the spatial configuration of these areas, on air quality regulation service has still no consensus. This configuration can affect air quality regulation services by altering the proximity between supply and demand areas, and thus affecting the extent of flows (METZGER *et al.*, 2021). Moreover, vegetation edges, created through fragmentation process, can increase pollutants deposition rate by wind interception, or on the contrary, they can act as physical barriers that prevent pollutants deposition in vegetation beyond the edges (IRGA; BURCHETT; TORPY, 2015). There are thus conflicting results, including some cases where higher fragmentation of green areas was associated with better air quality (SHI *et al.*, 2019; WU *et al.*, 2015), while other studies found that less fragmented areas present better air quality outcomes, probably because these areas have higher biomass or more structured vegetation (SHEN; LUNG, 2016, 2017).

Meteorological factors, as wind speed, can also affect air quality regulation flows, i.e., the connection between pollutants and greenspaces, because they determine pollutant's dilution and dispersion (OLENIACZ *et al.*, 2016) through their accumulation or ventilation (SEO *et al.*, 2018). Besides, dry deposition velocity is increased by wind speed, while it is negatively correlated with air humidity and air temperature (CHEN *et al.*, 2012; ODABASI; MUEZZINOGLU; BOZLAKER, 2002). Therefore, meteorological conditions also have an important effect on air quality regulation services (Figure 1).

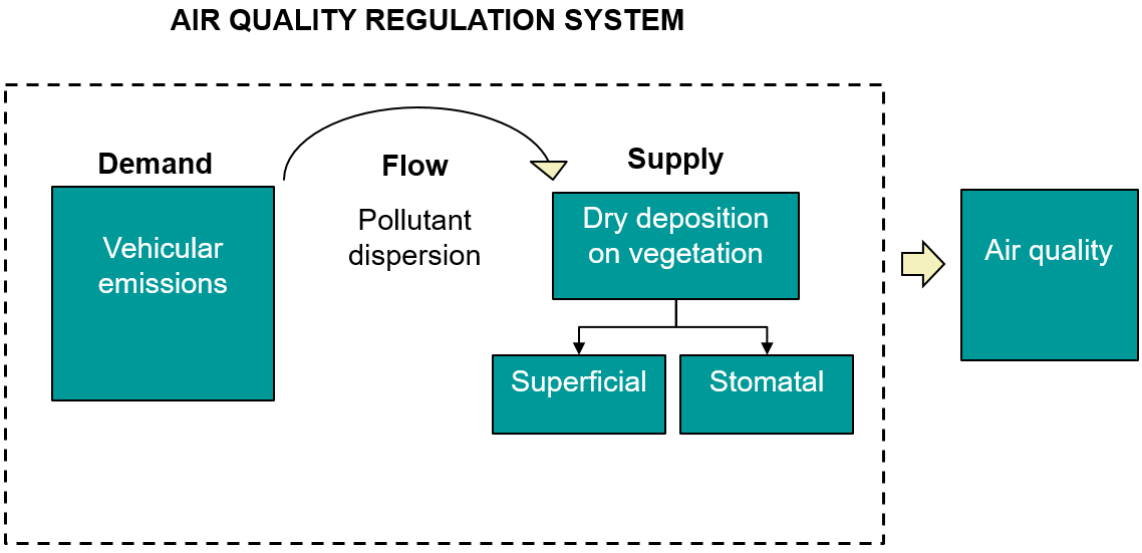

Figure 1. Simplified scheme showing the process of air quality regulation. Pollutants emitted by vehicles (here considered as demand) are dispersed in the air by wind (flow) and a fraction on this

is deposited on vegetation (supply areas). This process has an effect on air quality, diminishing pollutants concentrations.

The city of São Paulo, one of the biggest megacities in the world, is an interesting system to study the air quality regulation process given its high population density, high levels of air pollution, but also because it has a very extensive tree cover. High pollutant levels in the city are mainly caused by the vehicle fleet, which accounts for the emission of 96% of CO, 65% of NOx and 40% of PM (COMPANHIA AMBIENTAL DO ESTADO DE SÃO PAULO, 2020). Due to the social distancing imposed by COVID-19's quarantine from 22nd of March 2020, non-essential activities were restricted, and people were suggested to stay at home (decree Nº 64.881, March 20th). As a result, vehicular emissions were reduced during quarantine time, and so did pollutants concentrations of CO, NO2 and PM (DEBONE; COSTA; MIRAGLIA, 2020; FREITAS *et al.*, 2020). This offered a perfect scenario for us to also study the effect that an abrupt decay on demand (emissions) could have over the air regulation service.

Here we integrate the three components of air quality regulation (supply, demand, and flows) with meteorological factors with the aims to (1) analyze the potential of urban green areas to improve the air quality in the city of Sao Paulo; and (2) evaluate how the reduction in the demand during the COVID-19 quarantine affected the provision of this ecosystem service. We used vegetation's quantity, density, and spatial distribution (e.g., fragmentation) to estimate supply, vehicular emissions to estimate demand, and finally different spatial scales (spatial extent of analysis) to capture different scales or extents of pollutant flow, between emission and deposition areas.

We hypothesized that there is a positive effect of green areas over air quality and that this effect is enhanced with (Figure 2):

(i) Lower vehicular emissions (lower demand), since less emissions can avoid situations of overdemand (excessive demand);

(ii) A greater amount of green areas in the landscape (supply), because having more quantity of green areas will result in more biomass and therefore in pollutants deposition intensification;

(iii) A lower level of green areas fragmentation, because a lower fragmentation could lead to larger and more structured green areas, maximizing pollutant deposition.

Furthermore, we suppose that a reduction of demand in quarantine could enhance the air quality regulation service, since this alleviates problems of overdemand (Figure 2. ii)

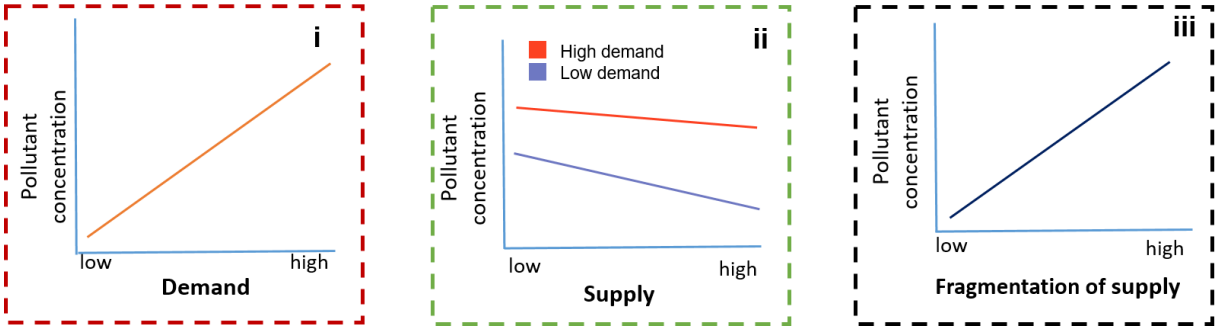

Figure 2. Schematic representation of the main hypotheses related to air quality regulation by green areas. This service should be affected by (i) the amount of demand (vehicular emissions; i), the supply (green areas) amount (ii) and fragmentation (iii), in addition to a demand effect on supply effectiveness (ii).

We expect our results to contribute to the discussion of air quality improvement in urban areas by providing guidance on how to better design urban greenspaces, both in amount and spatial configuration, being part of the solution for urban sustainability (Wu, 2010).

2 METHODOLOGY

2.1 Study area

The study area encompasses the city of São Paulo, the capital of São Paulo state, located in the southeast of Brazil (Figure 2). This megacity is the greatest of the southern hemisphere with an extension of 1.521 km^2 and a population of more than 12 million inhabitants (INSTITUTO BRASILEIRO DE GEOGRAFIA E ESTATÍSTICA, 2022). It is also the industrial and economical center of the country (accounts for 17% of its GDP; Silva-Sánchez, S., & Jacobi, 2014) and of South America. São Paulo is at an altitude of about 824 m, and its climate is classified as sub-tropical. This climate is characterized by a cold and dry season (April to September) with low humidity and reduced wind, and a warm and humid season (October to March) marked by high atmospheric temperatures (ANDRADE *et al.*, 2012, 2017). São Paulo is a relevant place to study air quality regulation service due to its central importance to Brazil´s economy, and given the large population affected by pollution problems.

Built-up areas represent 40% of the municipality, while 48% is covered by vegetation (being 40% tree cover), 8% of exposed soil, and 4% of water masses and dams (SECRETARIA MUNICIPAL DO VERDE E DO MEIO AMBIENTE, 2020). However, there is an unbalance distribution of greenspaces in the city since vegetation cover is reduced to 33% within urban city center (SECRETARIA MUNICIPAL DO VERDE E DO MEIO AMBIENTE, 2020), while large expanses of green areas are found around the city. Inside the urban matrix, vegetation cover is composed by fragments of secondary Atlantic forest, lowland formations, and natural fields, usually distributed in small parks, squares, and public roads. This vegetation is unequally distributed among the city's regions (AMATO-LOURENÇO *et al.*, 2016), with a higher concentration in the South (54.53%) and the North (41.67%), while the West (26.69%), East (16.04%), and center (15.56%) regions have more restricted green cover (SECRETARIA MUNICIPAL DO VERDE E DO MEIO AMBIENTE, 2020).

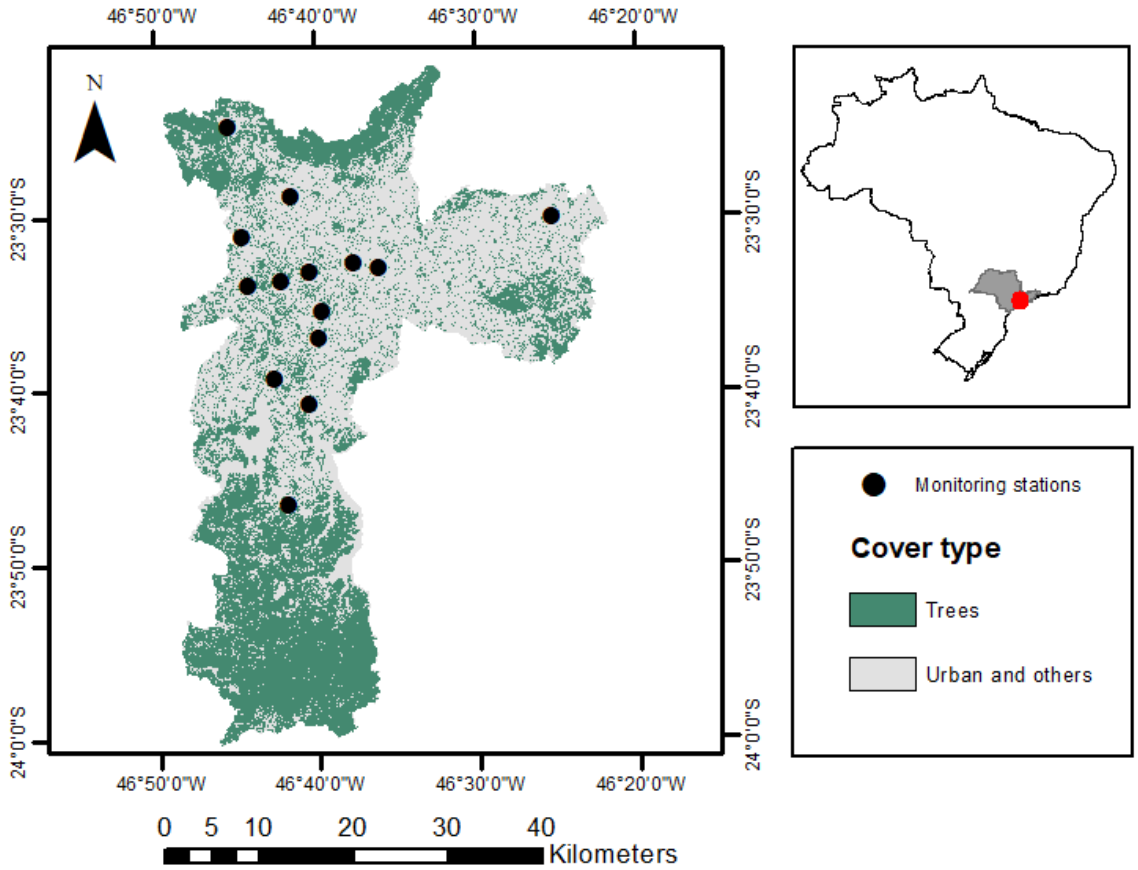

Figure 3. Spatial distribution of tree cover (green pixels), and urban and other type of areas (aquatic, pastures; grey pixels) in the city of São Paulo. Black dots represent the 14 CETESB's air quality monitoring stations included in the study. The small box on the right shows the location of São Paulo's city (red dot) within São Paulo's state (grey) and the country of Brazil (white).

2.2 Air pollution and meteorological data

For this study, we considered hourly air pollution data (CO, NO2, PM10, PM2.5) and meteorological data (e.g., wind velocity, air temperature, and relative humidity) from 14 automatic stations (study stations; see Figure 3 & Table S1) located within the city of Sao Paulo by using the QUALAR system of the CETESB (available at: https://qualar.cetesb.sp.gov.br/qualar/home.do). These data were obtained between 01/03/2020 and 31/05/2020 (period before and during COVID-19's quarantine) and were divided in three phases as follow: Pre-quarantine (01/03/2020 – 21/03/202), Quarantine A (22/03/20 -24/04/20), and Quarantine B (25/04/20 - 31/05/20). The first division was based on the quarantine start date (22nd of March 2020), and the division into the two quarantine periods was based on Google mobility trends ("COVID-19:

Relatórios de mobilidade da comunidade", 2022), which showed that the percentage of people staying at home decreased to its lowest mean value in the weekend of 25-04-20 to 26-04-20, since the beginning of quarantine (Table S2). Thus, Quarantine A was a more restrictive moment, when people were asked to stayed at home, agglomerations were prohibited, and only essential services were available to the public, while Quarantine B represents a more flexible moment of social distancing.

We extracted precipitation data to identify the days in which dry deposition occurred, and thus estimate the quantity of supply offered by tree cover around monitoring stations. We considered days with precipitation <0.2 mm as days in which dry deposition occurred (NOWAK *et al.*, 2013), and days with precipitation >0.2 mm as days with absence of the service. The precipitation data for each CETESB station coordinate was extracted from the Climate Hazards Group Infrared Precipitation with Station data (CHIRPS) of the University of California, with a spatial resolution of 0,05º (~5 km) and a daily temporal resolution.

2.3 Spatial scale (flow)

We used a multi-scalar approach to consider different flow capacities, i.e., the potential displacement of pollutants from their source. We thus defined different buffers around each monitoring station, creating different dimensions of interaction between supply and demand areas. We considered buffers of 250, 500, 750 and 1000 m of radii, since the influence of traffic-related air pollutants concentrations is considered to be of 100 m from a major urban road and of 500 m from a major freeway (HOEK *et al.*, 2008). We also created buffers of 750 and 1000 m once previous studies also found spatial effects at these scales on air regulation models (AGUILERA *et al.*, 2008; EEFTENS *et al.*, 2012; HOEK *et al.*, 2008; SMITH *et al.*, 2006). Even though particle dispersion can be even broader (more than 2069 m for PM10, and of 7726 m for PM2.5; Godoy, Mores, Cruz, & Scenna, 2009), 1000 m was the maximum scale possible for analysis, to avoid buffer overlapping among the stations included in our study.

2.4 Demand estimation

Knowing that the vehicle fleet is the most important contributor to São Paulo's air quality deterioration (COMPANHIA AMBIENTAL DO ESTADO DE SÃO PAULO, 2020), we modeled vehicular emissions as proxy of service demand. Hourly vehicular emission estimations were calculated using the VEIN R package, available at https://CRAN.R-project.org/package=vein, for the period between first March to 31 May 2020. VEIN uses traffic simulations obtained from the Traffic Engineering Company (CET http://www.cetsp.com.br/) and the Secretary of Transport and Mobility of São Paulo (SPtrans), available at http://www.sptrans.com.br/, to estimate vehicular emissions spatially. With this estimation, we extracted the mean hourly emissions of CO, NO2, and PM (10 and 2.5) around the 14 study areas, considering the different buffer sizes (scales) mentioned above.

2.5 Supply estimation

To estimate the amount of supply for the air regulation service, we first measured the amount of tree cover and the enhance vegetation index (EVI) for each buffer size. In order to do this, we used the 2020's vegetation cover mapping made by the city hall (available at: http://geosampa.prefeitura.sp.gov.br/PaginasPublicas/_SBC.aspx). The vegetation map was made in the years 2017/2018, covering the entire surface of the São Paulo municipality, including 1,168 km² in a scale of 1:1.000 and 359 km² in a scale 1:5.000 (SECRETARIA MUNICIPAL DO VERDE E DO MEIO AMBIENTE, 2020). The original map presents 15 different vegetation categories, which were grouped in 4 tree cover categories (low, medium, high, and very high; Figure 4 & Table S3).

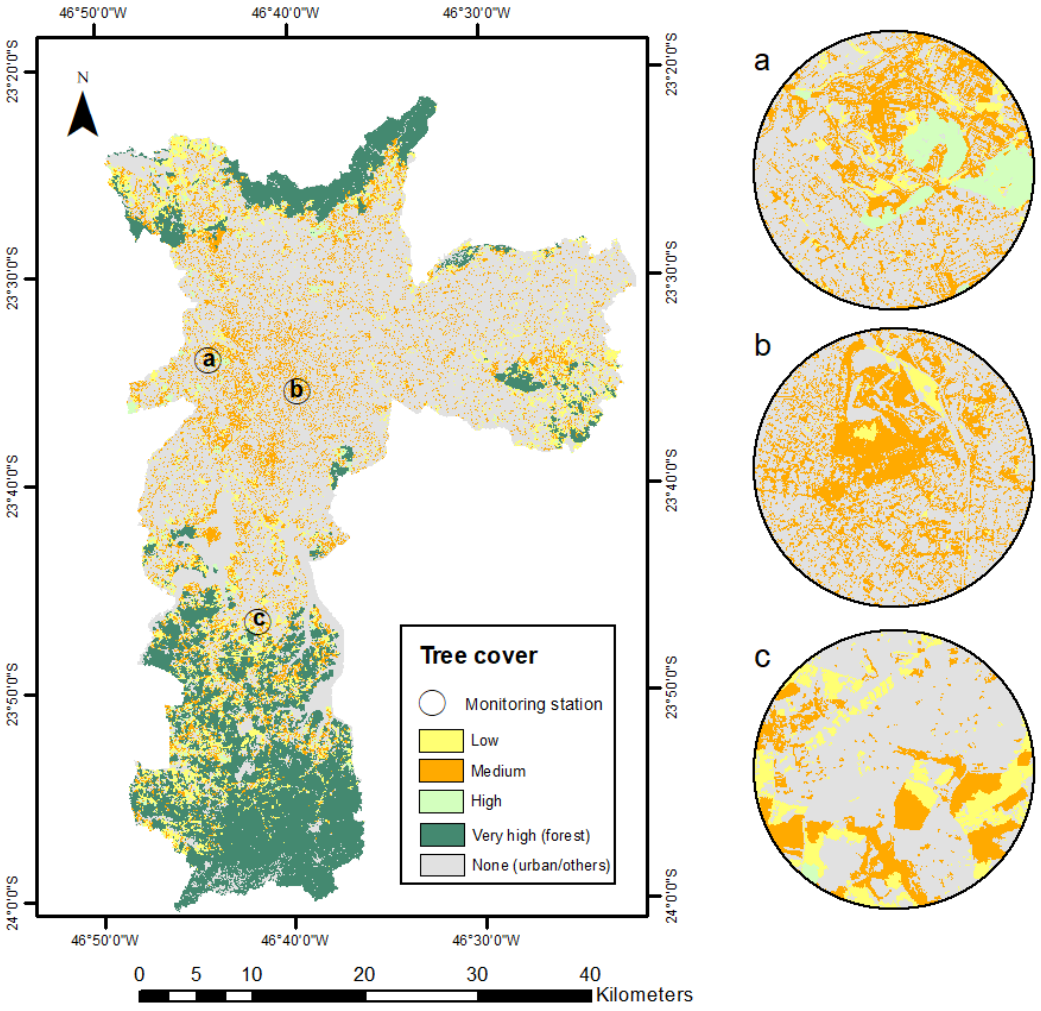

Figure 4. (a) Tree cover in the city of Sao Paulo: low, medium, high, and very high cover (primary forest and natural reserves); urban and others (aquatic, non-trees, forestry). (a-c) Close-up to buffers of 1000 m around different air quality stations: (a) Cidade Universitária-USP station (West zone); (b) Ibirapuera (South zone); (c) Grajaú-Parelheiros (South zone).

After obtaining the amount of tree cover by buffer around each station, we also measured the EVI, to include vegetation's density into our estimation of supply (see equation 2 below). EVI is sensitive to canopy structural variations (just like the leaf area index; LAI), which is important for air quality service regulation (ROELAND *et al.*, 2019). For EVI estimation, we used the Satveg site (https://www.satveg.cnptia.embrapa.br/satveg/), which uses the product MOD13Q1 (derived from the Terra satellite, starting on 02/18/2000) available in maximum compositions of 16 days, with a spatial resolution of approximately 250 m.

To finally estimate the air regulation supply service, we adapted the pollutant absorption formula proposed by Powe and Willis (2004) to a new supply formula:

Supply = A* EVI * DV * T * P $_{(0 \text{ or } 1)}$

Where: A is the total area of tree cover (including all types: low, medium, high, and very high cover; m2), EVI is the vegetation index value for the specific spatial scale, deposition velocity is the pollutant deposition rate from the UFORE-D model (Table S4; D. Nowak et al., 1998),T is the time step (seconds), and P is the daily precipitation value (0 when >= 0.02 mm and 1 when <= 0.02 mm; days with and without precipitation, respectively).

2.6 Configuration of supply

In order to analyze how the configuration of green areas could affect air quality, we extracted the number of patches (NP) of green areas (indicator of fragmentation) for each spatial scale analyzed. Landscapes with higher NP values are characterized by small, highly isolated patches with high edge proportions and low structural connectivity, being an indicative of ecosystem degradation based of landscape ecology principles (YUSHANJIANG *et al.*, 2018), and possibly of a reduction in ecosystem services.

2.7 Air regulation modelling

Before running a model selection approach, we performed a Mantel test to verify if there is a spatial correlation among pollution data within the 14 air quality stations. We made an independent test for each pollutant by creating a distance correlation matrix with the coordinates of each station and their corresponding mean concentration during the time of our study. We ran the test with 9999 permutations. The test revealed no spatial dependence ($p>0.05$ for all pollutants: PM10 = 0.54; PM2.5 = 0.85; NO2 = 0.30; CO= 0.60), with low correlation values for PM10 (-0.043), PM2.5 (-0.243), NO2 (0.068), CO (-0.107), validating the null hypothesis of spatial independence among air quality stations, for all pollutants.

In order to analyze the effect that an abrupt decay on emissions (demand) could have over the air regulation service's supply, we performed an ANOVA test considering the three categorical levels of the variable "quarantine" (Pre-quarantine, Quarantine A, and Quarantine B). A Tukey's test was used to identify which groups were different between each other.

To assess the relationship between pollutant concentrations and greenspaces, we performed a model selection approach. Model fitting was done using generalized linear mixed models with a negative binomial distribution. PM10, PM2.5, NO2 and CO were the response variables and we included the time of the day within each monitoring station (station: time_of_day), and the day of the week (i.e. Monday, Sunday…) as random effects. The predictor variables used were service's supply (hourly dry deposition by green areas), quarantine period (Pre-Quarantine, Quarantine A, and Quarantine B), demand (vehicular emissions), configuration of supply (number of green area patches), and meteorology data (relative humidity, wind velocity, and air temperature). Before running each subset of models, we conducted an exploratory data analysis to select only the explanatory variables with low correlation values (Pearson´s $r < 0.60$; Zuur, Ieno, Walker, Saveliev, & Smith, 2009).

Analyses were performed separately for each pollutant and subgrouping the models by spatial scales (250, 500, 750 and 1000 m), to consider different flow capacities of the pollutants. Models followed the structure: (1) supply: quarantine + (2) demand + (3) meteorological data (wind velocity, relative humidity, or air temperature; or combinations of relative humidity or air temperature with wind velocity; See Table S7) + (4) configuration of supply (number of patches). Supply, demand and meteorological variables were present in every model (See Table S7). In total, we considered 8 models by spatial scale (250 m, 500 m, 750 m, 1000 m of radii), for a total of 32 models for each pollutant (See Table S8).

Lastly, we conducted a maximum likelihood model selection procedure, considering the second order Akaike's information criteria, corrected for small sample sizes (AICc) (ANDERSON; BURNHAM, 2002). In this approach the lower the AICc, the better the model fits the data. All analyses were made with RStudio 1.4.1717, Fragstats v4.2.1 and ArcGIS 10.5.

Table 2. Parameters and data sources used to evaluate each of the variables present in the models.

Variable	Parameters	Data Source
Supply	▪ Green cover (m2)	▪ Geosampa
	▪ Enhance vegetation index (EVI)	▪ EVI index (MOD13Q1)
	▪ Deposition velocity for each pollutant (m/s)	▪ Deposition velocity (Nowak et al.,1998;2013).
	▪ Daily precipitation (0 or 1)	▪ CHIRPS
Demand	▪ Hourly vehicular emissions (g/km/h)	▪ VEIN model
Configuration of supply	▪ Number of vegetation patches (NP)	▪ Geosampa
Meteorology	▪ Air temperature ▪ Relative humidity ▪ Wind velocity	▪ CETESB
Air pollution	▪ CO, NO_2, ▪ PM10, PM2.5	▪ CETESB

3 RESULTS

3.1 Temporal patterns of pollutants, demand and supply

During the study period, the pollutants' concentrations varied widely, being generally highest in the pre-quarantine and Quarantine B periods; at the moment just after the start of the quarantine (A), all concentrations dropped considerably (Figure 5B & TableS2). The low pollutant concentrations were maintained in the first week of quarantine (days 22nd – 28th) but started to increase gradually after this period (days 29 - 35; Figure 5B), even exceeding pre-quarantine concentrations by the end of April - start of May (days 56 – 63; Figure 5B) and extending until the end of our study period.

NO2 and PM10 presented the highest mean values of daily concentrations, followed closely by PM2.5, while CO presented the lowest concentrations. Particularly, NO2 concentrations exceeded the recommended concentrations by the World Health Organization (WHO, 2021) both in periods A and C (25 µg/m3; See Table 3), while PM2.5 only exceeded the acceptable concentrations during period C (15 µg/m3). PM10 and CO mean daily concentrations were below the acceptable limits in all periods (45 µg/m3 and 4 µg/m3, respectively).

Vehicular emissions (demand) also showed a decline in the first week of lockdown, particularly in the case of PM10 and CO, and secondarily in the case of PM2.5. In contrast, NO2 emissions were low during all the study period. As observed with pollutants concentrations, emissions decreasing only lasted a few days (Figure 5C; days 22-28), and from the beginning of April (Day 32; Figure 5C) all pollutant emissions raised to values very close to the pre-quarantine period.

Finally, mean supply values given by the average hourly pollutant absorption of green areas, were higher and similar along the study period for PM2.5 and PM10, followed closely by NO2. Meanwhile, CO presented very low supply values (Figure 5D).

Table 3. Mean values by quarantine period for each pollutant, along with meteorological variables. Air quality guideline (AQG) values established by the OMS (values in bold are above daily air quality standards; World Health Organization, 2021).

Period		PM10 (µg/m3)	PM2.5 (µg/m3)	NO2 (µg/m)	CO (ppm)	Relative humidity (%)	Wind velocity (m/h)	Air temperature (°C)
	AQG	45.0	25.0	25.0	4.0			
A		22.6	12.0	**30.1**	0.5	76.5	1.8	21.8
B		21.4	11.2	22.1	0.4	74.4	1.9	20.1
C		33.9	**18.4**	**36.1**	0.8	70.2	1.6	17.9

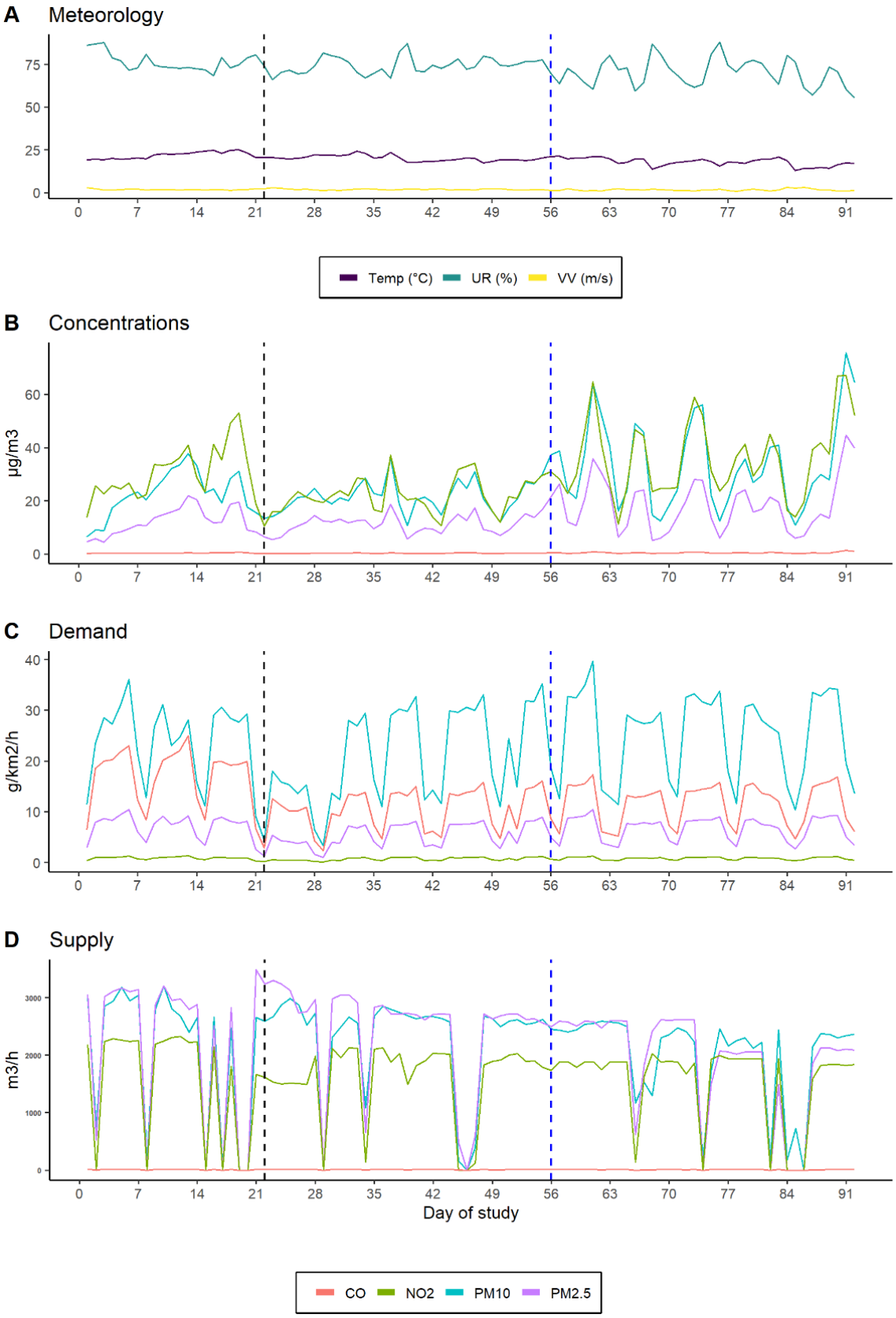

Figure 5. Mean daily variation in the data for: meteorological variables (TEMP= air temperature, UR= relative humidity, VV= wind velocity; A), pollutant concentrations (B), vehicular emissions

(C), and potential dry deposition by vegetation (D). Before the dashed black line are the days classified as pre-quarantine, between the black and blue dashed line are the days of Quarantine A, and after the blue line the days classified as Quarantine B. Supply values of 0 are from days with precipitation (days without dry deposition). Data in this figure is for the largest spatial scale (1000 m), which was the most commonly selected scale in the models.

3.2 Air quality regulation service

The best models selected (AICc < 2; Table 4) for all pollutants contained the interaction of supply with the quarantine period, demand, wind velocity, and relative humidity, and some of them additionally included the variable number of patches. The best scales of analysis ranged from 500 m to 1000 m, showing that interactions between supply and demand areas occur over wide territorial extents.

In general, meteorological variables had the highest effect on pollutants concentrations, followed by demand and supply along the quarantine periods (Figure 6). Demand (vehicular emissions) had a high positive effect on the observed NO2, CO, PM10, and PM2.5 concentrations, respectively. Supply only had a non-significant effect for PM2.5 during the Pre-quarantine period (Figure 6C-D). For all other pollutants it presented a significant effect, with larger effects for the quarantine A period (Figure 6A-B & 6E-H). In general, fragmentation (NP) had a positive effect on pollutants concentrations, with the exception of PM10, which showed non-significant effects (p=0.05). Finally, pollutants scale of dispersion (flow) for all pollutants was of 1000 m, except for PM2.5 for which the 500 m was selected.

Table 4. Results of the best selected models (ΔAICc ≤2) for each one of the pollutants evaluated.

Pollutant (Response variable)	Predictor Variables	Scale of effect	AICc	ΔAICc	df	weight
PM10 (a)	Supply: quarantine + Vehicular emissions + Relative humidity + Wind velocity+ Number of patches	1000 m	157678.2	0.0	12	0.582
PM10 (b)	Supply: quarantine + Vehicular emissions + Relative humidity+ Wind velocity	1000 m	157679.0	0.8	11	0.390
PM2.5 (a)	Supply: quarantine + Vehicular emissions + Relative humidity + Wind velocity	500 m	122553.1	0.0	11	0.402
PM2.5(b)	Supply: quarantine + Vehicular emissions + Relative humidity + Wind velocity + Number of patches	500 m	122554.1	1.0	12	0.245
NO2 (a)	Supply: quarantine + Vehicular emissions + Relative humidity + Wind velocity	1000 m	106328.8	0.0	13	0.69
NO2 (b)	Supply: quarantine + Vehicular emissions + Relative humidity + Wind velocity + Number of patches	1000 m	106330.5	1.6	14	0.31
CO (a)	Supply: quarantine + Vehicular emissions + Relative humidity + Wind velocity	1000 m	65979.2	0.0	13	0.68
CO (b)	Supply: quarantine + Vehicular emissions + Relative humidity + Wind velocity + Number of patches	1000 m	65980.7	1.5	14	0.32

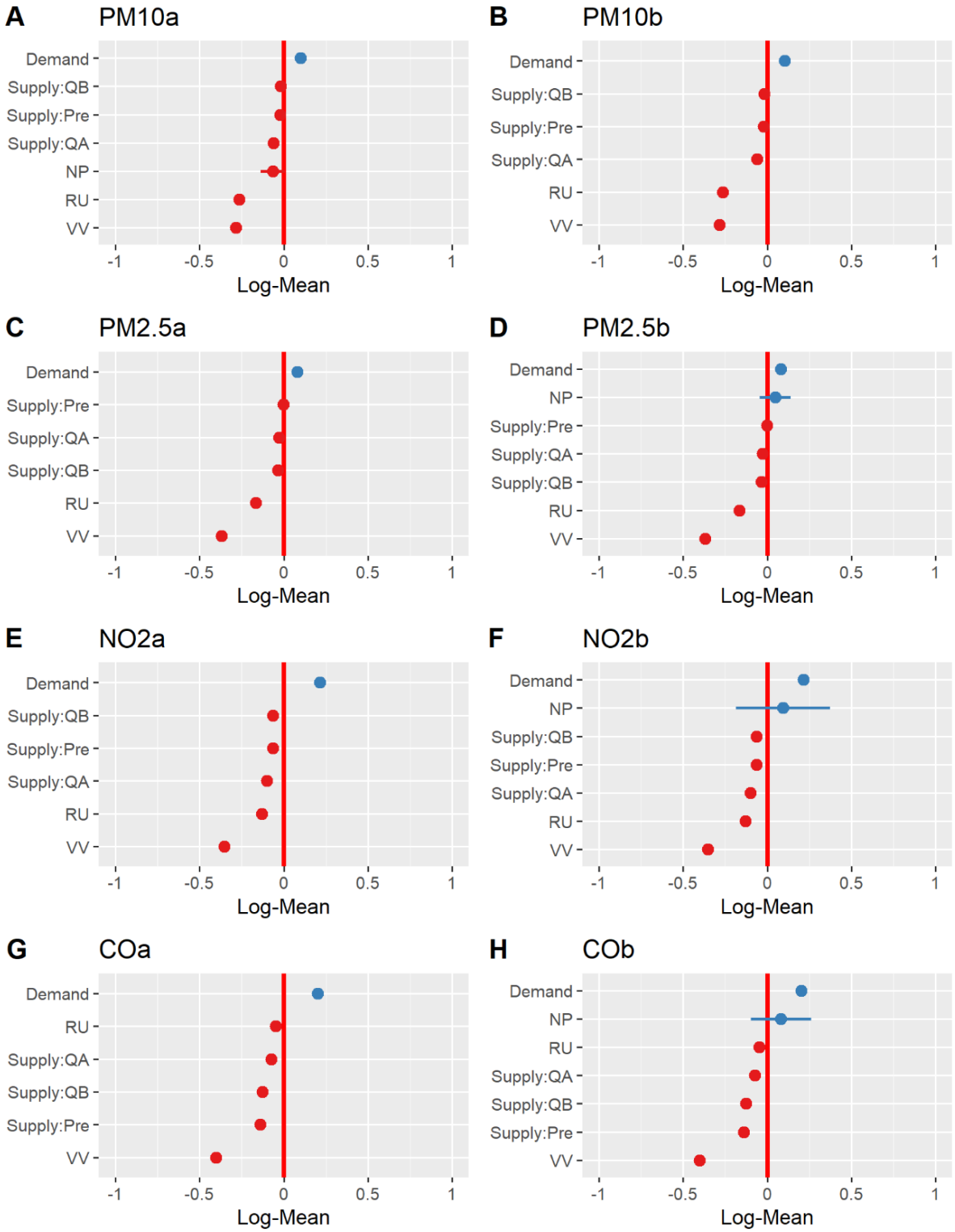

Figure 6. Parameter estimates of the variables present in the two best selected models (ΔAICc ≤2) for PM10 (A-B), PM2.5 (C-D), NO2 (E-F) and CO (G-H). Positive effects are shown in blue, while negative effects are shown in red. Coefficients whose confidence interval (horizontal lines) crosses the zero line are not significant. Demand= vehicular emissions, NP= number of patches, Supply: Pre= Effect of supply before quarantine, Supply: QA= effect of supply during quarantine A, Supply: QB = effect of supply during Quarantine B, WV = Wind velocity, RU=relative humidity.

3.2.1 PM10

Two models were equally plausible (ΔAICc ≤2) to explain the concentrations of PM10, both at the spatial scale of 1000 m. Both models contained the variables: supply by quarantine period, demand, wind velocity, and relative humidity; the best model additionally included the variable number of patches (Table 4). In general, number of patches (non-significant; p=0.05), supply by quarantine period, wind velocity, and relative humidity, had a negative effect on PM10 concentrations, while demand presented a positive effect over the response variable. According to our results, the variables with the highest effect to explain the observed patterns were wind velocity (-0.284), relative humidity (-0.265), demand (0.101), number of patches (-0.065), and supply during quarantine A (-0.060; Table 5).

Our results also showed that an increase in 1 m/h of wind velocity could result in a decrease of 6.3 µg/m3/h of PM10, while an increase of 20% in air humidity could result in a reduction of 6.0 µg/m3/h in the concentration of this pollutant. Concerning the demand, an increase in 29.0 g/km2/h in vehicle emissions could result in an increment of 2.5 µg/m3/h of PM10 concentrations. Having an extra 23 ha of tree cover (supply) could have an effect of decreasing 0.5 µg/m3/h of PM10 during the pre-quarantine period, 1.5 µg/m3/h during the quarantine period A, and 0.46 µg/m3/h during the quarantine B period. Finally, an increase of 33% in fragmentation (number of patches) could result in a decrease of 1.5 µg/m3/h on the pollutant air concentrations.

3.2.2 PM 2.5

Two models at the spatial scale of 500 m were equally plausible (ΔAICc ≤2) to explain PM2.5 concentrations. Both models included the variables: supply by quarantine period, demand, wind velocity and relative humidity; the second model additionally included the variable number of patches (Table 4). In general, the variables supply during quarantine A, supply during quarantine B, wind velocity, and relative humidity had a negative effect on PM2.5 concentrations, while demand and number of patches (fragmentation) presented positive effects. For this pollutant, supply during pre-quarantine period also had a negative but non-significant effect (p >0.05). According to our results, the variables with the highest effect to explain the observed patterns were wind velocity (-0.370), relative humidity (-0.165), demand (0.079), supply during quarantine B (-0.033) and supply during quarantine A (-0.027; Table 5).

Our models indicated that by increasing in 1 m/h the wind velocity could result in a reduction of 4 µg/m3/h of PM.5, and by increasing in 17% the air humidity could reduce in 1.96 µg/m3/h in the concentrations of this pollutant. An increase in 11 g/km2/h in the vehicle emissions also showed an increment of 1.1 µg/m3/h in the PM2.5 concentrations, while having an extra 15.7 ha of tree cover (supply) could decrease in 0.006 µg/m3/h of PM2.5 during the pre-quarantine period, 0.34 µg/m3/h during the quarantine period A, and 0.43 µg/m3/h during the quarantine B period.

Table 5: Slope and Standard Error (±SE) of every predictor variable present in the best models (∆AICc ≤ 2) selected to explain pollutant concentrations of PM10 and PM2.5.

	PM10		**PM2.5**	
Predictor variables	**Slope**	**(±SE)**	**Slope**	**(±SE)**
WV	-0.284	0.005	-0.370	0.006
RH	-0.265	0.006	-0.165	0.007
Demand(1000)	0.101	0.008		
Demand(500)			0.079	0.010
NP(1000)	-0.065	0.036		
Supply(1000):Pre	-0.020	0.009		
Supply(500):Pre			-0.000	0.012
Supply(1000):QA	-0.060	0.008		
Supply(500):QA			-0.027	0.011
Supply(1000):QB	-0.018	0.009		
Supply(500):QB			-0.033	0.012

3.2.3 NO2

Two models were equally plausible (ΔAICc ≤2) to explain NO2 concentrations, both at the spatial scale of 1000 m. Both models contained the variables: supply by quarantine period, demand, wind velocity, and relative humidity; the second model additionally included the variable number of patches (Table 4). In general, supply by quarantine period, wind velocity, and relative humidity had a negative effect on the response variable, while demand and number of patches had a positive effect. According to our results, the variables with the highest effect to explain the observed patterns were wind velocity (-0.353), demand (0.214), relative humidity (-0.128), and supply during quarantine A (-0.101; Table 6).

Our models also indicated that by increasing in 1 m/h the wind velocity, NO2 could present reductions of 7.52 µg/m3, while an increase of 17% in the relative humidity could reduce it by 3.0 µg/m3. For the demand, an increase in 0,7 g/km2/h in the emissions of the pollutant could result in an increase of 6.2 µg/m3 in its concentrations, while having an extra 32 ha of tree cover (supply) could decrease in 2.43 µg/m3 its concentrations during the quarantine A period, and in 1.49 µg/m3 during the periods of higher demand (pre-quarantine and quarantine B).

3.2.4 CO

Two models were equally plausible (ΔAICc ≤2) to explain the concentrations of the pollutant, with the best spatial scale selected being the 1000 m. Both models included the variables: supply by quarantine period, demand, wind velocity and relative humidity; the second model additionally included the variable number of patches. In general, supply by quarantine period, wind velocity, and relative humidity had a negative effect on CO concentrations, while demand and number of patches presented positive effects. According to our results, the variables with the highest effect to explain the observed patterns were wind velocity (-0.402), demand (0.200), supply during pre-quarantine (-0.140), and supply during quarantine B (-0.126; Table 6).

Our models also suggest that an increase in 1.6 m/h in wind speed could decrease in 0.11 ppm of CO, while an increase in 18% of relative humidity could result in a reduction in 0.01 ppm in pollutant concentrations. By raising in 12 g/km2/h in the pollutant emissions could also increase its concentrations by 0.07 ppm, while an extra

45 ha of tree cover (supply) could result in a decrease of 0.045 ppm during the pre-quarantine, 0.025 ppm during the quarantine A period and 0.041 ppm during the quarantine B period.

Table 6: Slope and Standard Error (±SE) of every predictor variable present in the best models (∆AICc ≤ 2) selected to explain pollutant concentrations of NO2 and CO.

	NO2		CO	
Predictor Variables	**Slope**	**(±SE)**	**Slope**	**(±SE)**
WV	-0.353	0.004	-0.402	0.005
RH	-0.128	0.005	-0.048	0.006
Demand (1000)	0.214	0.007	0.200	0.008
NP(1000)	0.093	0.142	0.081	0.091
Supply(1000):Pre	-0.064	0.008	-0.140	0.010
Supply(1000):QA	-0.101	0.009	-0.074	0.010
Supply(1000):QB	-0.064	0.008	-0.126	0.010

3.3 Effects of quarantine on air regulation service

We found differences in air pollutants concentrations among the three periods evaluated ($p<0.05$) through the ANOVA test, which were confirmed by the post-hoc test (Tukey test; $p<0.05$).

Our results showed that the direction and strength of the effect of the supply on pollutants concentration were depended on variations in the demand (pollutant emissions) caused by the COVID-19's quarantine. The increase in the strength of the negative effect of supply during the first days of the quarantine period (except for CO),

suggests that the supply service for PM10, PM2.5 and NO2 is enhance with a reduction in the demand (pollutants emissions).

When comparing the effects of supply in the three periods analyzed, all pollutants concentrations tended to decrease with higher supply values (amount of green areas), and this effect was intensified during the period of lower demand (quarantine A; green line in Figure 7). This effect was stronger for PM10 and NO2. For PM2.5, there was almost no effect of supply before the quarantine (red line; Figure 7 B), while PM10, NO2, and CO presented similar negative effects of supply during pre-quarantine and quarantine B periods (Figure 7 A-C-D). Finally, CO presented a slightly reduced effect of supply during quarantine A, probably because of its low deposition rate in vegetation along with the reduced concentrations of the pollutant during this period.

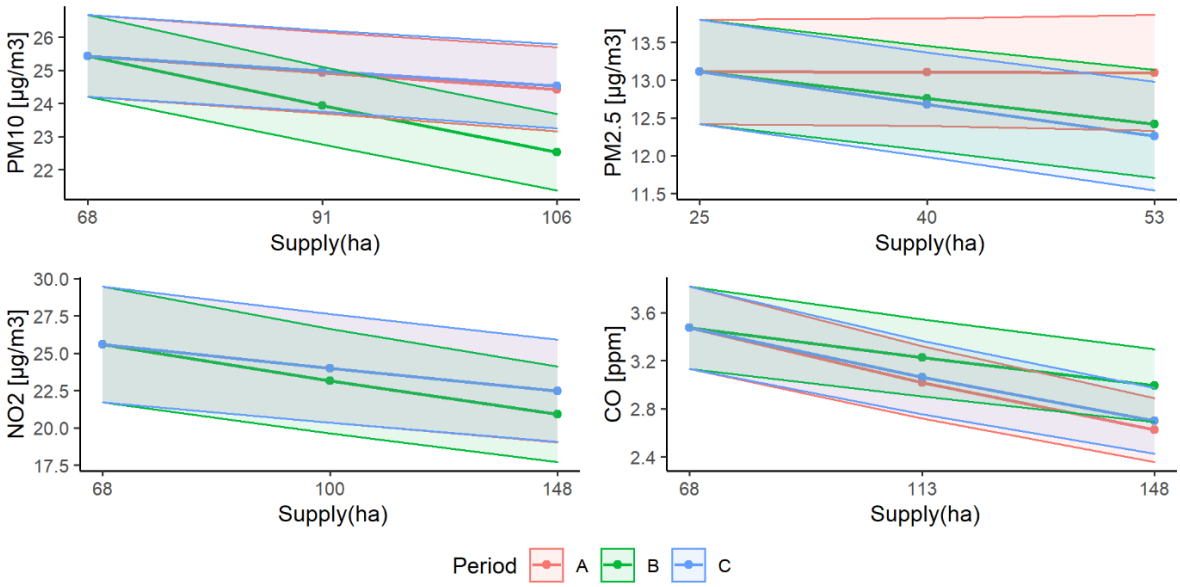

Figure 7. Effects of supply on pollutants concentrations depending on quarantine time. Periods were defined as: A= Pre-quarantine; B=First part of quarantine (more restrictive); C= Last part of quarantine (more flexible). PM10, NO2 and CO values of supply are higher since their spatial scale is of 1000 m, while PM2.5's is of 500 m.

4 DISCUSSION

To our knowledge, this study is the first to quantify the potential effects of urban green areas configuration on the air quality regulation service in tropical areas, using an approach of supply, demand and flow and during an atypical time (COVID-19's quarantine). Our results demonstrate that an increase in the amount of urban green areas and a reduction in vehicular emissions could contribute to air quality amelioration (especially of NO2 and PM10). In addition, our results point to the existence of a synergetic effect between the reductions in vehicular emissions and an increase in the provision of the service during the initial quarantine period, which may double the effect of supply reducing NO2 concentrations and triple the reduction on PM10 concentrations, compared to pre-quarantine time. Configuration of green areas (e.g., fragmentation) was not a significant factor for air pollution regulation. However, higher number of vegetation patches was related to higher concentrations of PM2.5, NO2 and CO, and to lower PM10 concentrations. Considering the overall trend of fragmentation impairing air quality regulation, we suggest the maintenance or expansion of existing green areas in cities for the mitigation of air pollution, especially in areas with a distance up to 1000 meters of the pollution source, since spatial scales of 500 and 1000 m of radii explained better pollutants concentrations. Higher wind velocities and relative humidity were also related with lower pollutants concentrations.

Vehicular emissions is one of the main contributors of air quality deterioration worldwide (ANENBERG *et al.*, 2015; FARIDI *et al.*, 2021; KUMAR *et al.*, 2021), negatively impacting human health (KIM; KABIR; KABIR, 2015; LAUMBACH; KIPEN, 2012; SONG *et al.*, 2019; WORLD HEALTH ORGANIZATION, 2017; ZHANG; BATTERMAN, 2013). Traffic related emissions alone are responsible for 11.7% of global PM 2.5 and ozone mortality (ANENBERG *et al.*, 2015), and in tropical growing cities constitute the main causes of premature mortality (ANDRADE *et al.*, 2012, 2017; VOHRA *et al.*, 2022).

Our results showed that a reduction in vehicle emissions could be responsible for significant air quality improvement, corroborating other studies (DEBONE; COSTA; MIRAGLIA, 2020; FREITAS *et al.*, 2020; FU; PURVIS-ROBERTS; WILLIAMS, 2020; KRECL *et al.*, 2020; NAKADA; URBAN, 2020). According to our model, this effect was

stronger for NO2 and CO concentrations. A similar result was also found in São Paulo (Debone et al., 2020; Krecl, Targino, Oukawa, & Casino Junuior, 2020; Nakada & Urban, 2020), where vehicular emissions contributed to NOx and CO reductions during the COVID-19 quarantine period.

The relationship between the presence and quantity of green areas and air quality improvement was established previously, even for tropical areas (ARROYAVE-MAYA *et al.*, 2019; BONILLA-BEDOYA *et al.*, 2021; JIM; CHEN, 2008; REYNOLDS *et al.*, 2017; RIBEIRO *et al.*, 2021; VAILSHERY; JAGANMOHAN; NAGENDRA, 2013). In Asia, for example, areas with higher tree covers presented increased pollutant removal (JIM; CHEN, 2008), while in South America, the presence of urban trees could capture almost 5000 kg/m2/year of pollutants (RIBEIRO *et al.*, 2021). However, a novelty of our study is that this effect can be exacerbated by reduction in demand (pollutant emissions), and may also be affected by the configuration of these green areas.

Here we show in an unprecedented way the effects of quarantine on the provision of air quality regulation service. We observed an intensification of the service in the period of less demand (less vehicular emissions/quarantine) for almost all pollutants (except CO), which resulted in an increase in the provision of the service in comparison with periods with more demand (overdemand; periods before and after quarantine). These variations in service provision may be explained by a decreasing in ecological pressures (pollutant emissions), since it is documented that the natural capacity and delivery of a service can be affected when there is an excess of demand (SCHEFFER; CARPENTER, 2003; VILLAMAGNA; ANGERMEIER; BENNETT, 2013; XU *et al.*, 2022).

In addition, the observed increased in service provision varied among the different pollutants analyzed. PM10 presented the highest service effect during the first part of quarantine (getting to triple pollutant's concentration reduction). This is partially related to its high deposition rate in vegetation (NOWAK *et al.*, 1998, 2013), which is higher than PM2.5's because larger particles are deposited more quickly than smaller particles (MCPHERSON; NOWAK; ROWNTREE, 1994). The lack of reduction in PM2.5 concentrations during pre-quarantine, even in areas with high values of supply, which contrasts with its strong reduction during quarantine, shows how much overdemand affected the provision of regulation service for this pollutant. This might

indicate a potential limit/threshold for the deposition of pollutants in vegetation, due to increased ecological pressures (overdemand) that affect the service's capacity by augmenting the requirement of ecological processes needed to meet this extra demand (VILLAMAGNA; ANGERMEIER; BENNETT, 2013). Furthermore, the enhancement of service for PM2.5 during the last part of quarantine could be due to temperature decline, because: (i) high temperatures affect the formation of PM2.5 by promoting photochemical reactions with precursors (CHEN *et al.*, 2017; WANG; OGAWA, 2015), and the period B of quarantine presented lower temperatures, which could have led to a diminish in concentrations and therefore to less ecological pressure for the delivery of the service; (ii) dry deposition of particles was found to be more effective at lower temperatures (CHEN *et al.*, 2017).

In the case of gaseous pollutants, service regulation had a high effect on NO2, probably because NO2 is captured within leaf stomata and is converted in nitrate ions that participate in protein build up (CIESLIK; OMASA; PAOLETTI, 2009; MCPHERSON; NOWAK; ROWNTREE, 1994), and thus is not resuspended as PM10 and PM2.5. In addition, the service effect on this pollutant was strongly enhanced (doubled) during the first part of quarantine, indicating that vehicular emissions in normal conditions (accountable for nearly 65% of NOx emissions; Companhia Ambiental do Estado de São Paulo, 2020) can lead to an overdemand situation. With the reduction in mobility caused by social distance, we saw experimentally how demand affects the potential service that could be offered by green areas (VILLAMAGNA; ANGERMEIER; BENNETT, 2013). Lastly, the slightly higher effect of supply for CO during periods of more demand, could be due to its low deposition rate (0.002 m s^{-1}), which probably increased a little when there were more concentrations of the pollutant in the air. Other modelling studies also found relationships between the decline of PM, CO, NO2 and the increase of greenspaces (BONILLA-BEDOYA *et al.*, 2021; PUGH *et al.*, 2012; ZOU *et al.*, 2016).

The configuration of green areas (fragmentation) appeared to be not as efficient as the amount of tree cover for air pollutant regulation, being not significant. Our results indicated a potential negative effect on air quality service, with larger fragmentation being related with higher concentrations of PM2.5, NO2 and CO. This could indicate that air quality regulation services are maximized by urban green areas that have lower fragmentation. The negative effect of fragmentation on air quality was

found for all pollutants with the exception of PM10. A hypothesis for this result is that edge areas could enhance PM10 flow and the exchange between greenspaces and the neighboring patches, increasing dry deposition (Wu et al., 2015). Furthermore, PM10 is a pollutant of big size which allows it to stay in the superficies where it deposits. In that way a larger fragmentation of urban greenspaces could be serving as nearby sinks for PM10 sources (streets).

Our results for NO2, CO and PM2.5, are consistent with previous findings that showed that minimizing fragmentation contributes to a reduction in air pollution (Jaafari, Shabani, Moeinaddini, Danehkar, & Sakieh, 2020; Mears, Brindley, Jorgensen, Ersoy, & Maheswaran, 2019; Shen & Lung, 2016, 2017). This may be because smaller patches are highly vulnerable to loss of species and functions (MILLENNIUM ECOSYSTEM ASSESSMENT, 2005), causing the weakened of provisioning, regulating, supporting, and cultural ecosystem services in rural and urban areas (JIANG *et al.*, 2022; QI *et al.*, 2013; YUSHANJIANG *et al.*, 2018)

However, other studies found lower PM2.5 concentrations associated with more even and scattered greenspaces patches (Shi et al., 2019; Wu et al., 2015). Therefore, the literature shows contrasting results about the effect of greenspace's fragmentation over air quality. Here, despite fragmentation not having a significant effect, it was selected in our model selection, indicating that overall, less fragmented areas are able to maximize the provision of the air regulation service. In the future, efforts should be made to increase data collection in a wider range of urban conditions and study scales to obtain clearer evidence for the adverse effect of fragmentation on the air regulation service.

Our results also indicate that air quality regulation service can occur in areas with a distance up to 1000 m from the pollution source. Our multiscale approach indicated that flow may be occurring in a scale of 500 m for PM2.5, and of 1000 m for NO2, CO and PM10, which may be related to meteorological variables. Wind velocity, which affects the transports air pollutants, presented positive effects in our models, suggesting that this variable can lead to a dispersion of the pollutants by kilometers (SEO *et al.*, 2018), reducing locally pollutants concentrations (IRGA; BURCHETT; TORPY, 2015; YANG *et al.*, 2020; ZHANG *et al.*, 2015), and potentially also affecting the scale of effect of service provision (LIU; FAN; DING, 2016).

However, the efficiency of flow also depends on the presence of obstacles which can slowdown or prevent the upward movement of pollutants by wind (buildings, topography, street canyons; Liu et al., 2016; Pugh et al., 2012; Ulpiani, Anne, Di, & Maharaj, 2022) making difficult its arrival to vegetation and favoring their accumulation. Relative humidity also showed a negative effect on pollutants concentrations in our and in other studies (HART *et al.*, 2021; KAYES *et al.*, 2019; LI *et al.*, 2014). This is explained by the fact that higher relative humidity favors dry deposition by increasing particle size and thus, rising its deposition rate (MOHAN, 2016; WU *et al.*, 2018).

It is worth mentioning that our estimations have limitations since we calculated pollutant absorption with average deposition rates found for studies made in the northern hemisphere, which count with a different plant composition. This estimates also assume an average wind velocity within their calculations of deposition, and although we include wind velocity, air humidity and air temperature as covariates, the average rates used might be underestimating the regulation service offered by urban green areas.

Concluding remarks and implications

This study provides evidence that green areas contribute to the amelioration of air quality in the city of São Paulo. In particular, we provide new evidence that the provision of air regulation service is enhanced by a greater amount of green areas in a less fragmented condition and by decreases in demand (pollutants emissions). Since the flows of pollutants can be extensive, beyond 1000 m, the maintenance of green areas, even away from the sources of pollution, can be relevant to the control of pollution as a whole.

Our results suggest that it is important to protect large green areas inside or nearby urban areas. In the case of São Paulo city, the protection of the already existing big green areas located at the extremes of the city can significantly contribute to the improvement of air quality in the city, and thus to the prevention of pollution-related diseases. Even though the more fragmented configuration is not ideal, the increase of green areas dispersed throughout the city acts as an increase in supply, which significantly affects the reduction of pollution. Finally, the provision of air quality regulation service can increase up to three times more in periods of reduced demand. So, in order to maintain pollutants concentrations within acceptable limits for human health, the ideal would be to both reduce vehicular emissions (demand) and increment the amount of green areas (supply) within the city.

References

AGUILERA, I.; SUNYER, J.; FERNÁNDEZ-PATIER, R.; HOEK, G.; AGUIRRE-ALFARO, A.; MELIEFSTE, K.; BOMBOI-MINGARRO, M. T.; NIEUWENHUIJSEN, M. J.; HERCE-GARRALETA, D.; BRUNEKREEF, B. Estimation of outdoor NO x, NO2, and BTEX exposure in a cohort of pregnant women using land use regression modeling. **Environmental science & technology**, v. 42, n. 3, p. 815–821, 2008.

AMATO-LOURENÇO, L. F.; MOREIRA, T. C. L.; ARANTES, B. L. D.; SILVA FILHO, D. F. D.; MAUAD, T. Metrópoles, cobertura vegetal, áreas verdes e saúde. **Estudos avançados**, v. 30, n. 86, p. 113–130, 2016.

ANDERSON, D. R.; BURNHAM, K. P. Avoiding pitfalls when using information-theoretic methods. **The Journal of wildlife management**, p. 912–918, 2002.

ANDRADE, M. D. F.; DE MIRANDA, R. M.; FORNARO, A.; KERR, A.; OYAMA, B.; DE ANDRE, P. A.; SALDIVA, P. Vehicle emissions and PM 2.5 mass concentrations in six Brazilian cities. **Air Quality, Atmosphere & Health**, v. 5, n. 1, p. 79–88, 2012.

ANDRADE, M. D. F.; KUMAR, P.; DIAS DE FREITAS, E.; YNOUE, R.; MARTINS, J.; MARTINS, L. D.; NOGUEIRA, T.; PEREZ-MARTINEZ, P.; DE MIRANDA, R. M.; ALBUQUERQUE, T.; TEIXEIRA, F. L.; OYAMA, B.; ZHANG, Y. Air quality in the megacity of São Paulo: Evolution over the last 30 years and future perspectives. **Atmospheric Environment**, v. 159, p. 66–82, 2017.

ANENBERG, S.; MILLER, J.; HENZE, D.; MINJARES, R. **A global snapshot of the air pollution-related health impacts of transportation sector emissions in 2010 and 2015**. Washington, DC: International Council on Clean Transportation (ICCT), 2015.

ARROYAVE-MAYA, M. del P.; POSADA-POSADA, M. I.; NOWAK, D. J.; HOEHN, R. E. Remoción de contaminantes atmosféricos por el bosque urbano en el valle de Aburrá Air pollution removal by the urban forest in the Aburra Valley. **Colombia Forestal**, v. 22, n. 1, p. 5–16, 2019.

BARÓ, F.; PALOMO, I.; ZULIAN, G.; VIZCAINO, P.; HAASE, D.; GÓMEZ-BAGGETHUN, E. Mapping ecosystem service capacity , flow and demand for landscape and urban planning : A case study in the Barcelona metropolitan region. **Land Use Policy**, v. 57, p. 405–417, 2016.

BECKETT, K. P.; FREER-SMITH, P. H.; TAYLOR, G. Particulate pollution capture by urban trees: effect of species and windspeed. **Global change biology**, v. 6, p. 995–1003, 2000.

BONILLA-BEDOYA, S.; ZALAKEVICIUTE, R.; MEJÍA, D.; DURANGO-CORDERO, J.; MOLINA, J. R.; MACEDO-PEZZOPANE, J. E.; HERRERA, M. Á. Spatiotemporal variation of forest cover and its relation to air quality in urban Andean socio-ecological systems. **Urban Forestry & Urban Greening**, v. 59, n. February, 2021.

CHEN, L.; LIU, C.; ZHANG, L.; ZOU, R.; ZHANG, Z. Variation in tree species ability to capture and retain airborne fine particulate matter (PM2.5). **Scientific Reports**, v. 7, n. April 2016, p. 1–11, 2017.

CHEN, L.; PENG, S.; LIU, J.; HOU, Q. Dry deposition velocity of total suspended particles and meteorological influence in four locations in Guangzhou , China. **Journal of Environmental Sciences**, v. 24, n. 4, p. 632–639, 2012.

CHOURABI, H.; GIL-GARCIA, J. R.; PARDO, T. A.; SCHOLL, H. J.; WALKER, S.; NAHON, K. Understanding Smart Cities : An Integrative Framework. In: 2012 45th Hawaii International Conference on System Sciences, 2012, [...]. IEEE, 2012. p. 2289–2297.

CIESLIK, S.; OMASA, K.; PAOLETTI, E. Why and how terrestrial plants exchange gases with air. **Plant Biology**, v. 11, n. 1948, p. 24–34, 2009.

COMPANHIA AMBIENTAL DO ESTADO DE SÃO PAULO. **Qualidade do ar no estado de São Paulo**. [s.l: s.n.]. Disponível em: <https://cetesb.sp.gov.br/ar/publicacoes-relatorios/>.

COVID-19: Relatórios de mobilidade da comunidade. Disponível em: <https://www.google.com/covid19/mobility/>. Acesso em: 14 set. 2022.

DEBONE, D.; COSTA, M. V; MIRAGLIA, S. G. E. K. 90 days of COVID-19 social distancing and its impacts on air quality and health in São Paulo, Brazil. **Sustainability**, v. 12, n. 18, p. 1–16, 2020.

EEFTENS, M.; BEELEN, R.; HOOGH, K. De; BELLANDER, T.; CESARONI, G.; CIRACH, M.; DECLERCQ, C.; DE, A.; DONS, E.; NAZELLE, A. De; DIMAKOPOULOU, K.; ERIKSEN, K.; FISCHER, P.; GALASSI, C.; GRAZ, R.; HEINRICH, J.; HO, B.; JERRETT, M.; KEIDEL, D.; KOREK, M.; LANKI, T.; LINDLEY, S.; MADSEN, C.; MO, A.; NA, G.; NIEUWENHUIJSEN, M.; NONNEMACHER, M.; PEDELI, X.; RAASCHOU-NIELSEN, O.; PATELAROU, E.; QUASS, U.; RANZI, Я. A.; SCHINDLER, Å. C.; STEMPFELET, M.; STEPHANOU, E.; SUGIRI, D.; TSAI, M.; YLI-TUOMI, T.; VARRO, J.; VIENNEAU, D.; KLOT, S. Von; WOLF, K.; BRUNEKREEF, B.; HOEK, G. Development of land use regression models for PM2.5, PM2.5 absorbance, PM10 and PM coarse in 20 European study areas; results of the ESCAPE project. **Environmental science & technology**, v. 46, n. 20, p. 11195–11205, 2012.

FARIDI, S.; YOUSEFIAN, F.; JANJANI, H.; NIAZI, S.; AZIMI, F.; NADDAFI, K.; SADEGH, M. The effect of COVID-19 pandemic on human mobility and ambient air quality around the world: a systematic review. **Urban Climate**, v. 38, n. May, p. 100888, 2021.

FREITAS, E. D.; IBARRA-ESPINOSA, S. A.; GAVIDIA-CALDERÓN, M. E.; REHBEIN, A.; RAFEE, S. A. A.; MARTINS, J. A.; MARTINS, L. D.; SANTOS, U. P.; NING, M. F.; ANDRADE, M. F.; TRINDADE, R. I. F. Mobility restrictions and air quality under COVID-19 pandemic in São Paulo, Brazil. n. April, p. 1–14, 2020.

FU, F.; PURVIS-ROBERTS, K. L.; WILLIAMS, B. Impact of the COVID-19 pandemic lockdown on air pollution in 20 major cities around the world. **Atmosphere**, v. 11, n. 2, 2020.

GODOY, S. M.; MORES, P. L.; CRUZ, A. S. M. S.; SCENNA, N. J. Assessment of impact distances for particulate matter dispersion : A stochastic approach. **Reliability Engineering & System Safety**, v. 94, n. 10, p. 1658–1665, 2009.

HART, M. A.; MAHARAJ, A. M.; DI VIRGILIO, G.; ULPIANI, G. Schools Weather and Air Quality (SWAQ) –Metadata – Urban Network, Sydney (NSW). 1 jul. 2021. Disponível em: <https://doi.org/10.5281/zenodo.5016296#.YyJyfozeKnE.mendeley>. Acesso em: 15 set. 2022.

HOEK, G.; BEELEN, R.; HOOGH, K. De; VIENNEAU, D.; GULLIVER, J.; FISCHER, P.; BRIGGS, D. A review of land-use regression models to assess spatial variation of outdoor air pollution. **Atmospheric Environment**, v. 42, p. 7561–7578, 2008.

INSTITUTO BRASILEIRO DE GEOGRAFIA E ESTATÍSTICA. **IBGE | Cidades@ | São Paulo | São Paulo | Panorama**. Disponível em: <https://cidades.ibge.gov.br/brasil/sp/sao-paulo/panorama>. Acesso em: 14 set. 2022.

IPCC. **Climate change 2014 mitigation of climate change. Contribution of working group III to the fifth sssessment report of the intergovernmental panel on climate change**. [s.l: s.n.].

IRGA, P. J.; BURCHETT, M. D.; TORPY, F. R. Does urban forestry have a quantitative effect on ambient air quality in an urban environment ? **Atmospheric Environment**, v. 120, p. 173–181, 2015.

JAAFARI, S.; SHABANI, A. A.; MOEINADDINI, M.; DANEHKAR, A.; SAKIEH, Y. Applying landscape metrics and structural equation modeling to predict the effect of urban green space on air pollution and respiratory mortality in Tehran. **Environmental Monitoring and Assessment**, v. 192, n. 7, p. 1–15, 2020.

JIANG, M.; JIANG, C.; HUANG, W.; CHEN, W.; GONG, Q.; YANG, J.; ZHAO, Y.; ZHUANG, C.; WANG, J.; YANG, Z. Quantifying the supply-demand balance of ecosystem services and identifying its spatial determinants : A case study of ecosystem restoration hotspot in Southwest China. **Ecological Engineering**, v. 174, n. April 2021, p. 106472, 2022.

JIM, C. Y.; CHEN, W. Y. Assessing the ecosystem service of air pollutant removal by urban trees in Guangzhou (China). **Journal of environmental management**, v. 88, n. 4, p. 665–676, 2008.

KAMPA, M.; CASTANAS, E. Human health effects of air pollution. **Environmental pollution**, v. 151, n. 2, p. 362–367, 2008.

KAYES, I.; SHAHRIAR, S. A.; HASAN, K.; AKHTER, M.; KABIR, M. M.; SALAM, M. A. The relationships between meteorological parameters and air pollutants in an urban environment. **Global Journal of Environmental Science and Management**, v. 5, n. 3, p. 265–278, 2019.

KIM, K.; KABIR, E.; KABIR, S. A review on the human health impact of airborne particulate matter. **Environment International**, v. 74, p. 136–143, 2015.

KRECL, P.; TARGINO, A. C.; OUKAWA, G. Y.; CASINO JUNUIOR, R. P. Drop in urban air pollution from COVID-19 pandemic: Policy implications for the megacity of São Paulo. **Environmental Pollution**, v. 265, n. January, p. 114883, 2020.

KRZYŻANOWSKI, M.; KUNA-DIBBERT, B.; SCHNEIDER, J. (Eds). **Health effects of transport-related air pollution**. [s.l.] WHO Regional Office Europe, 2005. https://news.ge/anakliis-porti-aris-qveynis-momava p.

KUMAR, P. G.; LEKHANA, P.; TEJASWI, M.; CHANDRAKALA, S. Effects of vehicular emissions on the urban environment- a state of the art. **Materials Today: Proceedings**, v. 45, p. 6314–6320, 2021.

LAUMBACH, R. J.; KIPEN, H. M. Respiratory health effects of air pollution: update on biomass smoke and traffic pollution. **Journal of allergy and clinical immunology**, v. 129, n. 1, p. 3–13, 2012.

LENZEN, M.; LI, M.; ARUNIMA, M.; POMPONI, F.; SUN, Y.; WIEDMANN, T.; FATURAY, F.; FRY, J.; GALLEGO, B.; GESCHKE, A. Global socio-economic losses and environmental gains from the Coronavirus pandemic. **PLoS ONE**, v. 15, n. 7, p. 1–13, 2020.

LI, L.; QIAN, J.; OU, C.-Q.; ZHOU, Y.-X.; GUO, C.; GUO, Y. Spatial and temporal analysis of air pollution index and its timescale-dependent relationship with meteorological factors in Guangzhou , China , 2001 - 2011. **Environmental Pollution**, v. 190, p. 75–81, 2014.

LIU, H. M.; FAN, Y. L.; DING, S. Y. Research progress of ecosystem service flow. **The Journal of Applied Ecology**, v. 27, n. 7, p. 2161–2171, 2016.

LIVESLEY, S. J.; MCPHERSON, E. G.; CALFAPIETRA, C. The urban forest and ecosystem services: impacts on urban water, heat, and pollution cycles at the tree, street, and city scale. **Journal of environmental quality**, v. 45, n. 1, p. 119–124, 2016.

LOH, H. C.; LOOI, I.; CH'NG, A. S.; GOH, K. W.; MING, L. C.; ANG, K. H. Positive global environmental impacts of the COVID-19 pandemic lockdown : a review. **GeoJournal**, v. 6, p. 1–13, 2021.

MCPHERSON, E. G.; NOWAK, D. J.; ROWNTREE, R. A. **Chicago's urban forest ecosystem: results of the Chicago Urban Forest Climate Project (Vol. 186)**. [s.l: s.n.].

MEARS, M.; BRINDLEY, P.; JORGENSEN, A.; ERSOY, E.; MAHESWARAN, R. Greenspace spatial characteristics and human health in an urban environment : An epidemiological study using landscape metrics in Sheffield , UK. **Ecological Indicators**, v. 106, n. June, p. 105464, 2019.

METZGER, J. P.; VILLARREAL-ROSAS, J.; SUÁREZ-CASTRO, A. F.; LÓPEZ-CUBILLOS, S.; GONZÁLEZ-CHAVES, A.; RUNTING, R. K.; HOHLENWERGER, C.; RHODES, J. R. Considering landscape-level processes in ecosystem service assessments. **Science of The Total Environment**, v. 796, 2021.

MILLENNIUM ECOSYSTEM ASSESSMENT, M. E. A. **Ecosystems and human well-being**. Washington, DC: Island press, 2005. 1–96 p.

MOHAN, S. M. An overview of particulate dry deposition : measuring methods , deposition velocity and controlling factors. **International journal of environmental science and technology**, v. 13, p. 387–402, 2016.

NAKADA, L. Y. K.; URBAN, R. C. COVID-19 pandemic: Impacts on the air quality during the partial lockdown in São Paulo state, Brazil. **Science of the Total Environment**, v. 730, p. 139087, 2020.

NOWAK, D. J.; HIRABAYASHI, S.; BODINE, A.; HOEHN, R. Modeled PM2.5 removal by trees in ten U.S. cities and associated health effects. **Environmental Pollution**, v. 178, p. 395–402, 2013.

NOWAK, D. J.; MCHALE, P.; IBARRA, M.; CRANE, D.; STEVENS, J. C.; LULEY, C. Modeling the effects of urban vegetation on air pollution. *In*: **Air pollution modeling and its application XII**. Boston, MA: Springer, 1998. p. 399–407.

ODABASI, M.; MUEZZINOGLU, A.; BOZLAKER, A. Ambient concentrations and dry deposition fluxes of trace elements in Izmir, Turkey. **Atmospheric Environment**, v. 36, p. 5841–5851, 2002.

OLENIACZ, R.; BOGACKI, M.; SZULECKA, A.; RZESZUTEK, M.; MAZUR, M. Assessing the impact of wind speed and mixing-layer height on air quality in Krakow (Poland) in the years 2014–2015. **Journal of civil engineering, environment and architecture**, v. 63, p. 315–342, 2016.

PAOLETTI, E.; KARNOSKY, D. F.; PERCY, K. E. Urban trees and air pollution. *In*: KONIJNENDIJK, C. C.; SCHIPPERIJN, J.; HOYER, K. K. **Forestry serving urbanised societies. IUFRO world series, volume 14**. Vienna, Austria: IUFRO Headquarters, 2004. p. 407.

POPESCU, F.; IONEL, I. Anthropogenic air pollution sources. **Air quality**, p. 1–22, 2010.

PUGH, T. A. M.; MACKENZIE, A. R.; WHYATT, J. D.; HEWITT, C. N. Effectiveness of green infrastructure for improvement of air quality in urban street canyons. **Environmental science & technology**, v. 46, 2012.

QI, Z.; XIN-YUE, Y.; ZHANG, H.; YU, Z.-L. Land fragmentation and variation of ecosystem services in the context of rapid urbanization: the case of Taizhou city, China. **Stochastic environmental research and risk assessment**, v. 28, n. 4, p. 843–855, 2013.

REYNOLDS, C. C.; ESCOBEDO, F. J.; CLERICI, N.; ZEA-CAMAÑO, J. Does “greening” of neotropical cities considerably mitigate carbon dioxide emissions? The case of Medellin, Colombia. **Sustainability**, v. 9, n. 5, 2017.

RIBEIRO, A.; BOLLMANN, H. A.; DE OLIVEIRA, A.; RAKAUSKAS, F.; CORTESE, T.; RODRIGUES, M.; QUARESMA, C.; FERREIRA, M. L. The role of tree landscape to reduce effects of urban heat islands : a study in two Brazilian cities. **Trees**, p. 1–14, 2021.

RIEDIKER, M.; CASCIO, W. E.; GRIGGS, T. R.; HERBST, M. C.; BROMBERG, P. A.; NEAS, L.; WILLIAMS, R.; DEVLIN, R. B. Particulate matter exposure in cars is associated with cardiovascular effects in healthy young men. **American journal of respiratory and critical care medicine**, v. 169, n. 8, p. 934–940, 2004.

ROELAND, S.; MORETTI, M.; AMORIM, J. H.; BRANQUINHO, C.; FARES, S.; MORELLI, F.; CALFAPIETRA, C. Towards an integrative approach to evaluate the environmental ecosystem services provided by urban forest. **Journal of Forestry Research**, v. 30, n. 6, p. 1981–1996, 2019.

ROY, S.; BYRNE, J.; PICKERING, C. A systematic quantitative review of urban tree benefits , costs , and assessment methods across cities in different climatic zones. **Urban Forestry & Urban Greening**, v. 11, n. 4, p. 351–363, 2012.

SCHEFFER, M.; CARPENTER, S. R. Catastrophic regime shifts in ecosystems : linking theory to observation. **Trends in ecology & evolution**, v. 18, n. 12, p. 648–656, 2003.

SECRETARIA MUNICIPAL DO VERDE E DO MEIO AMBIENTE. **Mapeamento digital da cobertura vegetal do município de São Paulo**. [s.l: s.n.].

SEO, J.; PARK, D. R.; KIM, J. Y.; YOUN, D.; LIM, Y. Bin; KIM, Y. Effects of meteorology and emissions on urban air quality : a quantitative statistical approach to long-term records (1999 – 2016) in Seoul, South Korea. **Atmospheric Chemistry and Physics**, v. 18, p. 16121–16137, 2018.

SHEN, Y.; LUNG, S. C. Can green structure reduce the mortality of cardiovascular diseases ? **Science of the Total Environment**, v. 566, n. 128, p. 1159–1167, 2016.

SHEN, Y.; LUNG, S. C. Mediation pathways and effects of green structures on respiratory mortality via reducing air pollution. **Scientific Reports**, v. 7, n. January, p. 1–9, 2017.

SHI, Y.; REN, C.; LAU, K. K.; NG, E. Investigating the influence of urban land use and landscape pattern on PM2 .5 spatial variation using mobile monitoring and WUDAPT. **Landscape and Urban Planning**, v. 189, n. April, p. 15–26, 2019.

SILVA-SÁNCHEZ, S., & JACOBI, P. R. Implementation of riverside parks in the city of São Paulo – progress and constraints. **Local Environment: The International Journal of Justice and Sustainability**, v. 21, n. October, p. 65–84, 2014.

SMITH, L.; MUKERJEE, S.; GONZALES, M.; STALLINGS, C.; NEAS, L.; NORRIS, G.; ÖZKAYNAK, H. Use of GIS and ancillary variables to predict volatile organic compound and nitrogen dioxide levels at unmonitored locations. **Atmospheric Environment**, v. 40, n. 20, p. 3773–3787, 2006.

SONG, J.; ZHAO, C.; LIN, T.; LI, X.; PRISHCHEPOV, A. V. Spatio-temporal patterns of traffic-related air pollutant emissions in different urban functional zones estimated by real-time video and deep learning technique. **Journal of Cleaner Production**, v. 238, p. 117881, 2019.

The Global Goals. Disponível em: <https://www.globalgoals.org/goals/11-sustainable-cities-and-communities/>. Acesso em: 14 set. 2022.

ULPIANI, G.; ANNE, M.; DI, G.; MAHARAJ, A. M. Urban meteorology and air quality in a rapidly growing city: inter-parameter associations and intra-urban heterogeneity. **Sustainable Cities and Society**, v. 77, n. November 2021, p. 103553, 2022.

VAILSHERY, L. S.; JAGANMOHAN, M.; NAGENDRA, H. Effect of street trees on microclimate and air pollution in a tropical city. **Urban Forestry & Urban Greening**, v. 12, n. 3, p. 408–415, 2013.

VILLAMAGNA, A. M.; ANGERMEIER, P. L.; BENNETT, E. M. Capacity , pressure , demand , and flow : A conceptual framework for analyzing ecosystem service provision and delivery. **Ecological Complexity**, v. 15, p. 114–121, 2013.

VOHRA, K.; MARAIS, E. A.; BLOSS, W. J.; SCHWARTZ, J.; MICKLEY, L. J.; DAMME, M. Van; CLARISSE, L.; COHEUR, P. Rapid rise in premature mortality due to anthropogenic air pollution in fast-growing tropical cities from 2005 to 2018. **Science Advances**, v. 8, n. April, 2022.

WANG, J.; OGAWA, S. Effects of meteorological conditions on PM2.5 concentrations in Nagasaki, Japan. **International Journal of Environmental Research and Public Health**, v. 12, n. 8, p. 9089–9101, 2015.

WEAGLE, C. L.; SNIDER, G.; LI, C.; DONKELAAR, A. Van; PHILIP, S.; BISSONNETTE, P.; BURKE, J.; JACKSON, J.; LATIMER, R.; STONE, E.; ABBOUD, I.; AKOSHILE, C.; ANH, N. X.; BROOK, R.; COHEN, A.; DONG, J.; GIBSON, M. D.; HE, K. B.; HOLBEN, B. N.; KAHN, R.; KELLER, C. A. Global sources of fine particulate matter: interpretation of PM2. 5 chemical composition observed by SPARTAN using a global chemical transport model. **Environmental science & technology**, v. 52, n. 20, p. 11670–11681, 2018.

WORLD HEALTH ORGANIZATION. **World health statistics 2017: monitoring health for the SDGs, Sustainable Development Goals.** Geneva: World Health Organization, 2017.

WORLD HEALTH ORGANIZATION. **WHO global air quality guidelines: particulate matter (PM2. 5 and PM10), ozone, nitrogen dioxide, sulfur dioxide and carbon monoxide. Executive summary**. Geneva: World Health Organization, 2021.

WU, J. Urban sustainability : an inevitable goal of landscape. **Landscape ecology**, v. 25, p. 1–4, 2010.

WU, J.; XIE, W.; LI, W.; LI, J. Effects of urban landscape pattern on PM2. 5 pollution—a Beijing case study. **PloS one**, v. 10, n. 11, p. 1–20, 2015.

WU, Y.; LIU, J.; ZHAI, J.; CONG, L.; WANG, Y.; MA, W.; ZHANG, Z.; LI, C. Comparison of dry and wet deposition of particulate matter in near-surface waters during summer. **PloS one**, v. 13, n. 6, p. 1–15, 2018.

XU, Z.; PENG, J.; DONG, J.; LIU, Y.; LIU, Q.; LYU, D. Spatial correlation between the changes of ecosystem service supply and demand : An ecological zoning approach. **Landscape and Urban Planning**, v. 217, n. February 2021, 2022.

YANG, J.; SHI, B.; SHI, Y.; MARVIN, S.; ZHENG, Y.; XIA, G. Air pollution dispersal in high density urban areas: Research on the triadic relation of wind, air pollution, and urban form. **Sustainable Cities and Society**, v. 54, p. 101941, 2020.

YUSHANJIANG, A.; ZHANG, F.; YU, H.; KUNG, H. Quantifying the spatial correlations between landscape pattern and ecosystem service value: A case study in Ebinur Lake Basin, Xinjiang, China. **Ecological Engineering**, v. 113, n. January, p. 94–104, 2018.

ZHANG, H.; XU, T.; ZONG, Y.; TANG, H.; LIU, X.; WANG, Y. Influence of meteorological conditions on pollutant dispersion in street canyon. **Procedia Engineering**, v. 121, p. 899–905, 2015.

ZHANG, K.; BATTERMAN, S. Air pollution and health risks due to vehicle traffic. **Science of the Total Environment**, v. 450, p. 307–316, 2013.

ZOU, B.; XU, S.; STERNBERG, T.; FANG, X. Effect of land use and cover change on air quality in urban sprawl. **Sustainability**, v. 8, n. 7, p. 677, 2016.

ZUUR, A. F.; IENO, E. N.; WALKER, N. J.; SAVELIEV, A. A.; SMITH, G. M. **Mixed effects models and extensions in ecology with R (Vol. 574)**. New York: Springer, 2009.

Appendices

Table S1. Pollutants measured by the CETESB in automatic stations included in the study.

Station name	CO	MP10	MP2.5	NO2
Cerqueira César	x	x		x
Cidade Universitária - USP - Ipen			x	
Congonhas	x	x	x	x
Grajau - Parelheiros	x	x	x	
Ibirapuera	x		x	x
Interlagos		x		
Itaim Paulista		x	x	x
Marginal Tietê - Ponte dos Remédios	x	x	x	x
Moóca	x		x	
Nossa Senhora do Ó		x		
Parque D. Pedro II	x	x	x	x
Perus		x	x	
Pinheiros	x		x	x
Santo Amaro	x	x		
N total	9	10	10	7

Table S2. Residential percentage (percentage of people who stayed at home) data from 01/03/2020 to 31/05/2020. Residential percentage (RP; percentage of people who stayed at home) data from 01/03/2020 to 31/05/2020 and by quarantine period. The higher the value, the higher the percentage of people who stayed at home. In bold are the values that correspond to the weekends.

Date	RP	Period
01/03/2020	**4**	A
02/03/2020	1	A
03/03/2020	1	A
04/03/2020	2	A
05/03/2020	2	A
06/03/2020	3	A
07/03/2020	**1**	A
08/03/2020	**1**	A
09/03/2020	2	A
10/03/2020	2	A
11/03/2020	2	A
12/03/2020	2	A
13/03/2020	2	A
14/03/2020	**1**	A
15/03/2020	**2**	A
16/03/2020	3	A
17/03/2020	7	A
18/03/2020	9	A
19/03/2020	12	A
20/03/2020	17	A
21/03/2020	**18**	A
22/03/2020	**17**	B
23/03/2020	23	B
24/03/2020	27	B

Date	RP	Period
25/03/2020	28	B
26/03/2020	27	B
27/03/2020	28	B
28/03/2020	**20**	B
29/03/2020	**18**	B
30/03/2020	25	B
31/03/2020	25	B
01/04/2020	26	B
02/04/2020	26	B
03/04/2020	27	B
04/04/2020	**19**	B
05/04/2020	**16**	B
06/04/2020	24	B
07/04/2020	24	B
08/04/2020	24	B
09/04/2020	22	B
10/04/2020	33	B
11/04/2020	**19**	B
12/04/2020	**15**	B
13/04/2020	23	B
14/04/2020	25	B
15/04/2020	25	B
16/04/2020	24	B
17/04/2020	25	B
18/04/2020	**18**	B
19/04/2020	**16**	B
20/04/2020	24	B
21/04/2020	30	B
22/04/2020	23	B

Date	RP	Period
23/04/2020	23	B
24/04/2020	24	B
25/04/2020	**17**	C
26/04/2020	**15**	C
27/04/2020	22	C
28/04/2020	23	C
29/04/2020	23	C
30/04/2020	20	C
01/05/2020	31	C
02/05/2020	**18**	C
03/05/2020	**15**	C
04/05/2020	21	C
05/05/2020	22	C
06/05/2020	23	C
07/05/2020	23	C
08/05/2020	23	C
09/05/2020	**16**	C
10/05/2020	**13**	C
11/05/2020	23	C
12/05/2020	23	C
13/05/2020	24	C
14/05/2020	24	C
15/05/2020	25	C
16/05/2020	**18**	C
17/05/2020	**16**	C
18/05/2020	22	C
19/05/2020	22	C
20/05/2020	26	C
21/05/2020	26	C

Date	RP	Period
22/05/2020	24	C
23/05/2020	**18**	C
24/05/2020	**16**	C
25/05/2020	27	C
26/05/2020	21	C
27/05/2020	22	C
28/05/2020	22	C
29/05/2020	21	C
30/05/2020	**14**	C
31/05/2020	**12**	C

Table S3. Original classification from the digital vegetation cover mapping made by SP city hall and the classification made for the present study (bold: not included in the study, e.g., non-arboreal vegetation or commercial monocultures).

Original classification	Code	Merged classification	Grouped categories	Arboreal category
Advanced Dense Ombrophilous Forest and Primary Dense Ombrophilous Forest	1	**Floating aquatic vegetation**	**8**	**1**
Middle-stage secondary dense ombrophilous forest	2	**Open vegetation (herbaceous-shrub)**	**6, 7, 12, 14**	**2**
Secondary dense ombrophilous forest at an early stage	3	Low arboreal	11	3
High montane dense ombrophilous forest (nebular forest)	4	Medium arboreal	13	4
Swampy and/or lowland forest	5	High arboreal	9	5
High mountain fields	6	**Sylviculture**	**10**	**6**
Lowland or marsh herbaceous-shrub vegetation	7	Forest	1, 2, 3, 4, 5, 15	7
Floating aquatic vegetation	8			
Heterogeneous forest massifs and urban forests	9			
Homogeneous forest massifs	10			
Low arboreal, arboreal-shrubby and/or arborescent cover	11			
Sylviculture	12			
Medium arboreal	13			
Herbaceous-shruby vegetation	14			
Mixed vegetation	15			

Table S4. UFORE-D estimates of total dry deposition to trees (Nowak et al.,1998; Nowak et al., 2013).

Pollutant	**Average deposition velocity (m s^{-1})**
PM10	0.0064
PM2.5	0.0043
NO2	0.0037
CO	0.00002

Table S5. Mean concentrations of PM10, PM2.5, CO and NO2 in the week before the start of quarantine period (Pre) and during the first week of the quarantine period (Quar) in each of the air quality monitoring stations of the municipality of São Paulo. There was a significant difference between the pollutant's concentrations before and during the first week of the quarantine ($p<0.05$; PM10=0.046; PM2.5=0.003; NO2= 0.002; CO=0.000).

Estação	**PM 10**		**PM 2.5**		**CO**		**NO2**	
	Pre	**Quar**	**Pre**	**Quar**	**Pre**	**Quar**	**Pre**	**Quar**
Cerqueira César	20.5	14.3	NA	NA	0.4	0.2	28	12.3
Cid.Universitária USP-IPEN	NA	NA	11.7	8.3	NA	NA	NA	NA
Congonhas	24.9	20.9	13.3	10.1	0.6	0.3	54.9	34.1
Grajaú-Parelheiros	26.0	19.5	11.6	8.17	0.4	0.2	NA	NA
Ibirapuera	NA	NA	9.4	6.6	0.3	0.1	19.7	15.7
Interlagos	17.1	16.4	NA	NA	NA	NA	NA	NA
Itaim Paulista	22.0	16.8	14.8	7.9	NA	NA	17.2	8.7
Marg.Tietê-Pte dos Remédios	27.5	19.2	17.9	9.9	0.6	0.2	55.8	26.9
Moóca	NA	NA	12.5	8.1	0.4	0.2	NA	NA
Nossa senhora do Ó	24.0	14.9	NA	NA	NA	NA	NA	NA
Parque D. Pedro II	20.1	18.3	15.6	16.5	0.2	0.0	29	15.9
Perus	24.1	31.7	12.5	10.9	NA	NA	NA	NA
Pinheiros	23.5	-	-	11.7	0.4	0.2	28.6	13.5
Santo Amaro	18.5	17.1	NA	NA	0.4	0.3	NA	NA

Table S6. Percentage of green cover around the 1000m buffer radii for each station. Total= total percentage of the buffer area with green cover; percentage of the total green cover that has low arboreal cover (Low), medium arboreal cover (Medium), high arboreal cover (High), and forest cover (Forest).

Stationname	Total	Low	Medium	High	Forest
Cerqueira César	29.14	5.01	94.99	0.00	0.00
Cid.Universitária USP-IPEN	44.89	13.30	60.89	25.81	0.00
Congonhas	16.34	10.42	89.58	0.00	0.00
Grajaú-Parelheiros	35.93	46.98	49.89	2.64	0.49
Ibirapuera	47.29	4.32	95.68	0.00	0.00
Interlagos	16.50	32.34	67.66	0.00	0.00
Itaim Paulista	14.83	48.51	51.49	0.00	0.00
Marg.Tietê-Pte dos Remédios	21.60	23.35	67.72	8.93	0.00
Moóca	11.82	8.78	91.22	0.00	0.00
Nossa senhora do Ó	10.51	23.99	76.01	0.00	0.00
Parque D. Pedro II	10.90	23.31	76.69	0.00	0.00
Perus	33.91	59.03	39.03	0.86	1.08
Pinheiros	31.82	7.32	92.68	0.00	0.00
Santo Amaro	19.37	44.02	55.98	0.00	0.0

Table S7. List of all models analyzed in the multiple regression analysis by pollutant and spatial scale. S= supply, Q= quarantine, D = demand, T= temperature, WV= wind velocity, RH= relative humidity, NP= number of patches.

Model Name	Pollutant (Response variable)	Predictor Variables	Scale
M1	PM10/ PM2.5/ NO2/ CO	Supply (S) : Quarantine (Q) + Demand (D) + Temperature (T)	1000, 750, 500, 250
M2	PM10/ PM2.5/ NO2/ CO	(S) : (Q) + (D) + Wind velocity (WV)	1000, 750, 500, 250
M3	PM10/ PM2.5/ NO2/ CO	(S) : (Q) + (D) + Relative humidity (RU)	1000, 750, 500, 250
M4	PM10/ PM2.5/ NO2/ CO	(S) : (Q) + (D) + (RU) + (WV)	1000, 750, 500, 250
M5	PM10/ PM2.5/ NO2/ CO	(S) : (Q) + (D) + (T) +(WV)	1000, 750, 500, 250
M6	PM10/ PM2.5/ NO2/ CO	(S) : (Q) + (D) + (WV) + (NP)	1000, 750, 500, 250
M7	PM10/ PM2.5/ NO2/ CO	(S) : (Q) + (D) + (T) + (WV) + (NP)	1000, 750, 500, 250
M8	PM10/ PM2.5/ NO2/ CO	(S) : (Q) + (D) + (RU) + (WV) + (NP)	1000, 750, 500, 250

Table S8. Results of models analyzed to explain concentrations of CO, NO2, PM10, and PM2.5. Only the best ten models selected for each pollutant are showed. S= supply, Q= quarantine, D = demand, T= temperature, WV= wind velocity, RH= relative humidity, NP= number of patches.

Model Name	Pollutant	Predictor variables	Scale	AICc	ΔAICc	df	Weight
M1	PM10	(S) : (Q) + (D) + (RU) + (WV) + (NP)	1000	157678.2	0.0	12	0.5823
M2	PM10	(S) : (Q) + (D) + (RU) + (WV)	1000	157679.0	0.8	11	0.3902
M3	PM10	(S) : (Q) + (D) + (RU) + (WV)	500	157685.1	6.9	11	0.0187
M4	PM10	(S) : (Q) + (D) + (RU) + (WV) + (NP)	500	157686.6	8.4	12	0.0089
M5	PM10	(S) : (Q) + (D) + (RU) + (WV)	750	157704.7	26.5	11	<0.001
M6	PM10	(S) : (Q) + (D) + (RU) + (WV) + (NP)	750	157705.3	27.0	12	<0.001
M7	PM10	(S) : (Q) + (D) + (RU) + (WV)	250	157713.7	35.5	11	<0.001
M8	PM10	(S) : (Q) + (D) + (RU) + (WV) + (NP)	250	157715.6	37.3	12	<0.001
M9	PM10	(S) : (Q) + (D) + (T) +(WV)	500	157715.6	37.3	12	<0.001
M10	PM10	(S) : (Q) + (D) + (T) + (WV) + (NP)	500	159191.6	1513.4	12	<0.001
M1	PM2.5	(S) : (Q) + (D) + (RU) + (WV)	500	122553.1	0.0	11	0.402
M2	PM2.5	(S) : (Q) + (D) + (RU) + (WV) + (NP)	500	122554.1	1.0	12	0.245
M3	PM2.5	(S) : (Q) + (D) + (RU) + (WV)	1000	122555.1	2.0	11	0.150

M4	PM2.5	(S) : (Q) + (D) + (RU) + (WV)	750	122555.8	2.7	11	0.102
M5	PM2.5	(S) : (Q) + (D) + (RU) + (WV) + (NP)	1000	122556.8	3.7	12	0.063
M6	PM2.5	(S) : (Q) + (D) + (RU) + (WV) + (NP)	750	122557.8	4.7	12	0.038
M7	PM2.5	(S) : (Q) + (D) + (RU) + (WV)	250	122568.2	15.1	11	<0.001
M8	PM2.5	(S) : (Q) + (D) + (RU) + (WV) + (NP)	250	122569.3	16.2	12	<0.001
M9	PM2.5	(S) : (Q) + (D) + (T) +(WV)	500	122880.0	326.9	11	<0.001
M10	PM2.5	(S) : (Q) + (D) + (T) + (WV) + (NP)	500	122880.6	327.5	12	<0.001
M1	NO2	(S) : (Q) + (D) + (RU) + (WV)	1000	107811.8	0.0	11	0.69
M2	NO2	(S) : (Q) + (D) + (RU) + (WV) + (NP)	1000	107813.4	1.6	12	0.31
M3	NO2	(S) : (Q) + (D) + (RU) + (WV)	750	107863.2	51.5	11	<0.001
M4	NO2	(S) : (Q) + (D) + (RU) + (WV) + (NP)	750	107864.8	53.0	12	<0.001
M5	NO2	(S) : (Q) + (D) + (RU) + (WV)	500	107995.0	183.2	11	<0.001
M6	NO2	(S) : (Q) + (D) + (RU) + (WV) + (NP)	500	107996.6	184.8	12	<0.001
M7	NO2	(S) : (Q) + (D) + (RU) + (WV)	250	108142.1	330.3	11	<0.001
M8	NO2	(S) : (Q) + (D) + (RU) + (WV) + (NP)	250	108144.1	332.3	12	<0.001

M9	NO2	(S) : (Q) + (D) + (T) +(WV)	1000	108274.7	462.9	11	<0.001
M10	NO2	(S) : (Q) + (D) + (WV)	1000	108275.2	463.4	10	<0.001
M1	CO	(S) : (Q) + (D) + (RU) + (WV)	1000	66991.4	0.0	11	0.65
M2	CO	(S) : (Q) + (D) + (RU) + (WV) + (NP)	1000	66992.6	1.2	12	0.35
M3	CO	(S) : (Q) + (D) + (T) +(WV)	1000	67010.2	18.8	11	<0.001
M4	CO	(S) : (Q) + (D) + (T) +(WV) + (NP)	1000	67011.3	19.9	12	<0.001
M5	CO	(S) : (Q) + (D) + (WV)	1000	67038.8	47.4	10	<0.001
M6	CO	(S) : (Q) + (D) + (WV) + (NP)	1000	67039.9	48.5	11	<0.001
M7	CO	(S) : (Q) + (D) + (RU) + (WV)	750	67079.9	88.5	11	<0.001
M8	CO	(S) : (Q) + (D) + (RU) + (WV) + (NP)	750	67080.4	89.0	12	<0.001
M9	CO	(S) : (Q) + (D) + (T) +(WV)	750	67104.1	112.7	11	<0.001
M10	CO	(S) : (Q) + (D) + (T) +(WV) + (NP)	750	67104.2	112.9	12	<0.001